Ref. Ares(2025)9477208 - 04/11/2025

www.icaria-project.eu

D2.4 ICARIA multi-hazards modelling tools and application guidelines - version 2

DRAFT

This project has received funding from the European Union's Horizon Europe research and innovation programme under grant agreement No. 101093806. The publication reflects only the authors' views and the European Union is not liable for any use that may be made of the information contained therein.

D2.4 ICARIA multi-hazards modelling tools and application guidelines – version 2

Summary

Deliverable 2.4 of ICARIA is an updated version Deliverable 2.3 that defines and generalises an adaptable framework to be adopted within the project for the setup and simulation of a variety of compound hazard events. The work within this deliverable summarises developments as part of Task 2.3 "Coupled hazard models: methodology and tool". Deliverable 2.4 further refines the methodologies and modelling tools developed in Deliverable 2.3 to provide an improved assessment. Within this task, a range of different multi-hazard scenarios have been assessed with details pertaining to how respective approaches and modelling tools can be utilised to model compound hazard scenarios. In addition this document also provides details on how climate data utilised within the compound hazard models can be assessed to derive joint probability distributions of compound hazard events.

The methodologies thus outlined within this document can serve as guidelines for the selection of input parameters and coupling of tools for multi-hazard assessment.

Deliverable number	Work package	
D2.4	WP2	
Deliverable lead beneficiary	**Deliverable author(s)**	**Contributor(s)**
UNEXE	Albert Chen, Barry Evans (UNEXE)	Lydia Vamvakeridou-Lyroudia (UNEXE), Dragan Savic (UNEXE) Alex de la Cruz Coronas (AQUA) Nadia Politi (DMKTS) Marianne Bügelmayer-Blaschek (AIT)
Internal reviewer(s)	**External reviewer(s)**	
Beniamino Russo (UPC)	Mattia Leone (UNINA)	
Planned delivery date	**Actual delivery date**	
	27/10/2025	
Dissemination level	☑ **PU = Public** ☐ PP = Restricted to other programme participants ☐ RE = Restricted to a group specified by the consortium. Please specify: _____ ☐ CO = Confidential, only for members of the consortium	

Document history

Date	Version	Author	Comments
03/10/2025	0.1	A Chen (UNEXE)	First Draft
05/10/2025	0.2	B Evans (UNEXE)	Adding methodology information
05/10/2025	1.0	A Chen (UNEXE)	Initial version of document prior to internal and external review
12/10/2025	2.0	A Chen (UNEXE)	Additional joint-probability assessment results included

This project has received funding from the European Union's Horizon Europe research and innovation programme under grant agreement No. 101093806. The publication reflects only the authors' views and the European Union is not liable for any use that may be made of the information contained therein.

20/10/2025	3.0	A Chen (UNEXE)	Further results on pluvial and storm surge compound events added. Peer review comments addressed.
27/10/2025	4.0	A Chen (UNEXE)	Further peer review comments addressed.

DRAFT

This project has received funding from the European Union's Horizon Europe research and innovation programme under grant agreement No. 101093806. The publication reflects only the authors' views and the European Union is not liable for any use that may be made of the information contained therein.

Table of contents

List of Figures 5

List of Tables 8

List of Acronyms and Abbreviations 10

Executive summary 8

1. Introduction 9

2. Objectives of deliverable 11

3. Generalised Compound Modelling Framework 13

3.1 Physical Model Interactions 13

3.1.1 Compound Coincident Hazards 16

3.1.2 Compound Consecutive Hazards 16

3.2 Joint Probability Assessment 17

3.2.1 Bivariate Copula Assessment 20

3.2.2 Bivariate Copula Assessment with Linear Regression 29

3.2.3 Multivariate Copula Assessment 30

4. Single Hazard Models Overview 31

5. Model Setup Guidelines 32

5.1 Flooding (Pluvial) and Storm Surge 32

5.1.1 Compound Model setup 32

5.1.2 Joint Probability Assessment 37

5.2 Flooding and Extreme Wind 48

5.2.1 Compound Model setup 48

5.2.2 Joint Probability Assessment 49

5.3 Extreme Wind and Forest Fire 52

5.3.1 Compound Model setup 52

5.3.2 Joint Probability Assessment 54

5.4 Drought and Heatwave 61

5.4.1 Compound Model setup 61

5.4.2 Joint Probability Assessment 62

5.5 Drought and Forest Fire 63

5.5.1 Compound Model setup 63

5.5.2 Joint Probability Assessment 64

5.6 Heatwave and Forest Fire 65

5.6.1 Compound Model setup 65

This project has received funding from the European Union's Horizon Europe research and innovation programme under grant agreement No. 101093806. The publication reflects only the authors' views and the European Union is not liable for any use that may be made of the information contained therein.

5.6.2 Joint Probability Assessment 65
5.7 Heatwave, Drought and Forest Fire 67
5.7.1 Compound Model setup 67
5.7.2 Joint Probability Assessment 67
6. Conclusions ***68***
6.1 Summary 68
6.2 Lessons learned 69
References ***71***
Annex 1: Data Management Statement ***74***

DRAFT

This project has received funding from the European Union's Horizon Europe research and innovation programme under grant agreement No. 101093806. The publication reflects only the authors' views and the European Union is not liable for any use that may be made of the information contained therein.

List of Figures

Figure 1. Summary of hazards and risk receptors considered in the different CS of ICARIA. 11

Figure 2. Spatial and temporal scales of 16 selected natural hazards, shown on logarithmic axes for spatial and temporal scales (Gill and Malamud, 2014). 13

Figure 3. Spatial and temporal scales of modelled hazards within ICARIA (adapted from Franzke, 2017). 14

Figure 4. Physical interactions between hazards. 15

Figure 5. Compound Coincident Hazards. 16

Figure 6. Compound Consecutive Hazards. 16

Figure 7. Schematic representation of consecutive disasters (de Ruiter et al., 2020). 17

Figure 8. Temporal depiction of compound coincident hazards at different time scale ranges. 19

Figure 9. Marginal distribution of daily rainfall and maximum wind speed for Salzburg baseline case [*Historical Data*]. 19

Figure 10. Marginal distribution of daily rainfall and maximum wind speed for Salzburg baseline case [*Synthetic Data*]. 21

Figure 11. The comparisons of the probability distribution functions of Daily rainfall (left) and Maximum wind speed (right). 21

Figure 12. Daily joint probability of daily rainfall and maximum wind speed combinations (points), and the derived annual joint probability contours for the (a) historical and (b) synthetic data under the baseline scenario. 22

Figure 13. Temporal depiction of compound consecutive hazards. 22

Figure 14. Daily joint probability of daily rainfall and maximum wind speed combinations (points), and the annual joint probability (contours) for 2071-2099 period under SSP 126 (left) and SSP 585 (right) scenarios for (a) compound events, (b) consecutive events within a 7-day time window (c) consecutive events within a 30-day time window. 23

Figure 15. Combined Joint Probability of SSPs 126, 245, 370, and 585 for (a) EC-EARTH3 climate model and (b) CanESM5 climate model. 24

Figure 16. Maximum wind speed for 1.1, 2, 5, 10, 30, 50, and 100 year return periods using 4 SSPs (126, 245, 370, and 585), each includes 6 climate models (ACCESS-CM2, CanESM5, CMCC-ESM2, CNRM-ESM2-1, EC-EARTH3, and MRI-ESM2-0). 25

Figure 17. Daily rainfall for 1.1, 2, 5, 10, 30, 50, and 100 year return periods using 4 SSPs (126, 245, 370, and 585), each includes 10 climate models (MPI-ESM1-2-HR, BCC-CSM2-MR, CanESM5, CMCC-ESM2, EC-EARTH3, NorESM2-MM, ACCESS-CM2, CNRM-ESM2-1, MRI-ESM2-0, and UKESM1-0-LL). 25

Figure 18. Marginal distribution of maximum wind speed and FWI for KOS in South Aegean Region (KOS) baseline (a) historical data (b) Synthetic data with bivariate Copula only. 29

Figure 19. Marginal distribution of maximum wind speed and FWI for South Aegean Region (KOS) baseline case [Synthetic data with bivariate Copula and linear regression]. 29

Figure 20. Multivariate Copula Analysis of maximum temperature, maximum wind speed and FWI for KOS in the South Agena Region (a) historical data (b) synthetic data. 30

This project has received funding from the European Union's Horizon Europe research and innovation programme under grant agreement No. 101093806. The publication reflects only the authors' views and the European Union is not liable for any use that may be made of the information contained therein.

Figure 21. Hazard Classifications being modelled within ICARIA. 31

Figure 22. Scheme of a sewer system and the sewer interceptor. 32

Figure 23. Conceptual model of the occurrence of backwater effect (Qiang et al., 2021a). 33

Figure 24. Flowchart of the one-way coupled approach to link pluvial flood and storm surge models. 34

Figure 25. Scheme of an outfall connected to the sea under different conditions: (a) normal operation in dry weather conditions, (b) CSO due to an extreme rain event; (c) coincident storm surge and CSO. 35

Figure 26. Scheme of a low-lying coastal area under different conditions: (a) dry weather conditions, (b) extreme rainfall conditions; (c) coincident coincidence storm surge and extreme rainfall conditions. 36

Figure 27. Temporal depiction of modelling of pluvial flood events during a storm surge. 37

Figure 26. Daily rainfall distribution for 10, 30, 50, and 100 year return periods and maximum using 4 SSPs (126, 245, 370, and 585), each includes 10 climate models (MPI-ESM1-2-HR, BCC-CSM2-MR, CanESM5, CMCC-ESM2, EC-EARTH3, NorESM2-MM, ACCESS-CM2, CNRM-ESM2-1, MRI-ESM2-0, and UKESM1-0-LL), for Barcelona region. 39

Figure 28. Q50 percentile storm surge and daily rainfall joint annual probability contours of (dependence measure $\rho = 0.1$) Barcelona under SSP 126 (left) and SSP 585 (right) for (a) 2015-2040, (b) 2041-2070, and (c) 2071-2100 period 42

Figure 29. Q90 percentile storm surge and daily rainfall joint annual probability contours (dependence measure $\rho = 0.1$) of Barcelona under SSP 126 (left) and SSP 585 (right) for (a) 2015-2040, (b) 2041-2070, and (c) 2071-2100 period 43

Figure 30. Q50 percentile storm surge and daily rainfall joint annual probability contours (dependence measure $\rho = 0.4$) of Barcelona under SSP 126 (left) and SSP 585 (right) for (a) 2015-2040, (b) 2041-2070, and (c) 2071-2100 period 44

Figure 31. Q90 percentile storm surge and daily rainfall joint annual probability contours of (dependence measure $\rho = 0.4$) Barcelona under SSP 126 (left) and SSP 585 (right) for (a) 2015-2040, (b) 2041-2070, and (c) 2071-2100 period 45

Figure 32. Q50 percentile storm surge and daily rainfall joint annual probability contours of (dependence measure $\rho = 0.7$) Barcelona under SSP 126 (left) and SSP 585 (right) for (a) 2015-2040, (b) 2041-2070, and (c) 2071-2100 period 46

Figure 33. Q90 percentile storm surge and daily rainfall joint annual probability contours (dependence measure $\rho = 0.7$) of Barcelona under SSP 126 (left) and SSP 585 (right) for (a) 2015-2040, (b) 2041-2070, and (c) 2071-2100 period 47

Figure 34. Temporal depiction of modelling of flood events during or following extreme wind. 49

Figure 35. Marginal distribution of daily rainfall and maximum wind speed for Salzburg under (a) SSP 126 and (b) SSP 585 scenarios (2071-2099]. 50

Figure 36. Daily joint probability of daily rainfall and maximum wind speed combinations (points), and the derived annual joint probability contours for the for Salzburg under SSP 126 (left) and SSP 585 scenarios (2071-2099] for (a) compound events, (b) consecutive events within a 7-day time window (c) consecutive events within a 30-day time window. 51

Figure 37. Structure of the FWI System (https://cwfis.cfs.nrcan.gc.ca/background/summary/fwi). 52

This project has received funding from the European Union's Horizon Europe research and innovation programme under grant agreement No. 101093806. The publication reflects only the authors' views and the European Union is not liable for any use that may be made of the information contained therein.

Figure 38. Temporal depiction of modelling influence of extreme wind on FWI scores. 54
Figure 39. Marginal probability distribution of daily wind speed and FWI data for KOS (left) and SYROS (right) in South Aegean Region under (a) baseline, (b) 2015-2040 period in SSP 126 and (c) 2015-2040 period SSP 585 scenarios. 60
Figure 40. Temporal depiction of modelling heatwaves during periods of drought. 62
Figure 41. Temporal depiction of modelling FWI scores during periods of drought. 64
Figure 42. Defining compound Heatwave with Wildfire scenario. 65
Figure 43. Defining compound Drought, Heatwave with Wildfire scenarios. 67

DRAFT

This project has received funding from the European Union's Horizon Europe research and innovation programme under grant agreement No. 101093806. The publication reflects only the authors' views and the European Union is not liable for any use that may be made of the information contained therein.

List of Tables

Table 1. Modelling approaches to coupling hazards (Santiago-Collazo et al., 2019). 15

Table 2. Information about the 10 climate models belonging to the 6 Coupled Model Intercomparison Project (CMIP6) corresponding to the IPCC AR6. Models were retrieved from the Earth System Grid Federation (ESGF) portal in support of the Program for Climate Model Diagnosis and Intercomparison (PCMDI) (Deliverable 1.2). 18

Table 3. The median estimation of 1.1, 2, 5, 10, 30 and 100 year return period wind gust within SLZ region derived from 4 SSPs (126, 245, 370, and 585), each includes 6 climate models (ACCESS-CM2, CanESM5, CMCC-ESM2, CNRM-ESM2-1, EC-EARTH3, and MRI-ESM2-0).26

Table 4. The 90th percentile estimation of 1.1, 2, 5, 10, 30 and 100 year return period wind gust within SLZ region derived from 4 SSPs (126, 245, 370, and 585), each includes 6 climate models (ACCESS-CM2, CanESM5, CMCC-ESM2, CNRM-ESM2-1, EC-EARTH3, and MRI-ESM2-0). 27

Table 5. The median estimation of 1.1, 2, 5, 10, 30 and 100 year return period wind gust within SLZ region derived from 4 SSPs (126, 245, 370, and 585), each includes 10 climate models (MPI-ESM1-2-HR, BCC-CSM2-MR, CanESM5, CMCC-ESM2, EC-EARTH3, NorESM2-MM, ACCESS-CM2, CNRM-ESM2-1, MRI-ESM2-0, and UKESM1-0-LL). 28

Table 6. The 90th percentile estimation of 1.1, 2, 5, 10, 30 and 100 year return period wind gust within SLZ region derived from 4 SSPs (126, 245, 370, and 585), each includes 10 climate models (MPI-ESM1-2-HR, BCC-CSM2-MR, CanESM5, CMCC-ESM2, EC-EARTH3, NorESM2-MM, ACCESS-CM2, CNRM-ESM2-1, MRI-ESM2-0, and UKESM1-0-LL). 28

Table 7. Extreme event definitions for modelled hazards. 31

Table 8. Main sources of uncertainty in the one-way coupled pluvial flooding and storm surge multi-hazard model and possible improvements. 37

Table 9. Median estimation of 1.1, 5, 10, 50, 100 and 500 year return period daily rainfall for Barcelona region under SSP 126 and SSP 585 scenarios. 38

Table 10. 90th percentile estimation of 1.1, 5, 10, 50, 100 and 500 year return period daily rainfall for Barcelona region under SSP 126 and SSP 585 scenarios. 38

Table 9. Median estimation of 1.1, 2, 5, 10, 30, 50, and 100 year return period daily rainfall for Barcelona region derived from 4 SSPs (126, 245, 370, and 585), each includes 10 climate models (MPI-ESM1-2-HR, BCC-CSM2-MR, CanESM5, CMCC-ESM2, EC-EARTH3, NorESM2-MM, ACCESS-CM2, CNRM-ESM2-1, MRI-ESM2-0, and UKESM1-0-LL) 40

Table 10. 90th percentile estimation of .1, 2, 5, 10, 30, 50, and 100 year return period daily rainfall for Barcelona region derived from 4 SSPs (126, 245, 370, and 585), each includes 10 climate models (MPI-ESM1-2-HR, BCC-CSM2-MR, CanESM5, CMCC-ESM2, EC-EARTH3, NorESM2-MM, ACCESS-CM2, CNRM-ESM2-1, MRI-ESM2-0, and UKESM1-0-LL) 40

Table 13. Classification of values for the FWI and the ISI according to EFFIS (https://forest-fire.emergency.copernicus.eu/about-effis/technical-background/fire-danger-forecast). 53

Table 14. The annual joint probability for maximum wind speed exceeding 40 km/h and FWI exceeding baseline daily 90th percentile thresholds for South Aegean Region for baseline, SSP 126 and SSP 585 scenarios. 55

This project has received funding from the European Union's Horizon Europe research and innovation programme under grant agreement No. 101093806. The publication reflects only the authors' views and the European Union is not liable for any use that may be made of the information contained therein.

Table 15. The annual joint probability for maximum wind speed exceeding baseline daily 90th percentile and FWI exceeding baseline daily 90th percentile thresholds for South Aegean Region for baseline, SSP 126 and SSP 585 scenarios. 56

Table 16. The annual joint probability for maximum wind speed exceeding baseline daily 95th percentile and FWI exceeding baseline daily 90th percentile thresholds for South Aegean Region for baseline, SSP 126 and SSP 585 scenarios. (casd09) 57

Table 17. The annual joint probability for maximum wind speed exceeding baseline daily 99th percentile and FWI exceeding baseline daily 90th percentile thresholds for South Aegean Region for baseline, SSP 126 and SSP 585 scenarios. (case11) 58

Table 18. The annual joint probability for both maximum wind speed and FWI exceeding baseline exceeding baseline 20% annual possibility thresholds for South Aegean Region for baseline, SSP 126 and SSP 585 scenarios. (case03) 59

Table 19. Drought classifications based on SPI. 61

Table 20. The annual joint probability with 3 or more consecutive days that temperature exceeding 95th percentile of recorded summer temperatures during the period of 1981 – 2010, followed by FWI exceeding the 90th percentile of historical period during 1981-2010 baseline. 66

DRAFT

This project has received funding from the European Union's Horizon Europe research and innovation programme under grant agreement No. 101093806. The publication reflects only the authors' views and the European Union is not liable for any use that may be made of the information contained therein.

List of Acronyms and Abbreviations

AMB	Barcelona Metropolitan Area
BUI	Buildup Index
CFFDRS	Canadian Forest Fire Danger Rating System
CI	Critical infrastructure
CMIP6	Coupled Model Intercomparison Project Phase 6
CS	Case study
CSO	Combined Sewer Overflow
DSS	Decision support system
FFMC	Fine Fuel Moisture Code
FWI	Fire Weather Index
HNMS	Hellenic National Meteorological Service
HW	Heat Waves
ISI	Initial Spread Index
LST	Land Surface Temperature
RAF	Resilience Assessment Framework
SAR	South Aegean Region
SLZ	Salzburg Region
SOLWEIG	SOlar and LongWave Environmental Irradiance Geometry model
SPI	Standardised Precipitation Index
SS	Storm Surge
SSPs	Shared Socioeconomic Pathways
SSO	Strategic Sub Objectives

This project has received funding from the European Union's Horizon Europe research and innovation programme under grant agreement No. 101093806. The publication reflects only the authors' views and the European Union is not liable for any use that may be made of the information contained therein.

Executive summary

This deliverable outlines the approaches being adopted within the ICARIA project for the modelling of compound hazard events across the three case study regions.

With global temperatures rising, it is anticipated that the likelihood and severity of single and compound hazards are going to increase. To plan for and mitigate against such events, it is apparent that a multi-hazard and multi-risk assessment is needed. Previous deliverables within WP2 outlined models and tools used for single hazard assessment across the three case study regions addressing a variety of climate driven hazards. These are then expanded on this further providing generalised overview of methods used for multi-hazard assessment and means of assessing the joint probability of compound hazard events.

The main objectives of this document can be summarised as follows:

- Provide a generalised framework for the depiction and modelling of compound hazards that includes their:
  - Physical interactions and,
  - Joint probabilities

- Provide guidelines to serve as exemplar for the physical modelling of a variety of compound hazard combinations that includes both compound coincident and compound consecutive hazards.

This project has received funding from the European Union's Horizon Europe research and innovation programme under grant agreement No. 101093806. The publication reflects only the authors' views and the European Union is not liable for any use that may be made of the information contained therein.

1. Introduction

The number of climate-related disasters has been progressively increasing in the last two decades and this trend could be drastically exacerbated in the medium- and long-term horizons according to climate change projections. It is estimated that, between 2000 and 2019, 7,348 natural hazard-related disasters have occurred worldwide, causing 2.97 trillion US$ losses and affecting 4 billion people (UNDRR, 2020). These numbers represent a sharp increase of the number of recorded disaster events in comparison with the previous twenty years. Much of this increase is due to a significant rise in the number of climate-related disasters (heatwaves, droughts, flooding, etc.), including compound events, whose frequency is dramatically increasing because of the effects of climate change and the related global warming. In the future, by mid-century, the world stands to lose around 10% of total economic value from climate change if temperature increase stays on the current trajectory, and both the Paris Agreement and 2050 net-zero emissions targets are not met.

In this framework, **Project ICARIA** has the overall objective to promote the definition and the use of a comprehensive asset level modelling framework to achieve a better understanding about climate related impacts produced by complex, compound and cascading disasters and the possible risk reduction provided by suitable, sustainable and cost-effective adaptation solutions.

This project will be especially devoted to critical assets and infrastructures that are susceptible to climate change, in a sense that its local effects can result in significant increases in cost of potential losses for unplanned outages and failures, as well as maintenance – unless an effort is undertaken in making these assets more resilient. ICARIA aims to understand how future climate might affect life-cycle costs of these assets in the coming decades and to ensure that, where possible, investments in terms of adaptation measures are made up front to face these changes.

To achieve this aim, ICARIA has identified 7 Strategic Sub Objectives (SSO), each one related to one or several work packages. They have been classified according to different categories: scientific, corresponding to research activities for advances beyond the state of the art (SSO1, SSO2, SSO3, SSO4, SO5); technological, suggesting and/or developing novel solutions, integrating state-of-the art and digital advances (SSO6); societal, contributing to improved dialogue, awareness, cooperation and community engagement as highlighted by the European Climate Pact (SSO7); and related to dissemination and exploitation, aimed at sharing ICARIA results to a broader audience and number of regions and communities to maximise project impact (SSO7).

1. SSO1.- Achievement of a comprehensive methodology to assess climate related risk produced by complex, cascading and compound disasters
2. SSO2.- Obtaining tailored scenarios for the case studies regions
3. SSO3.- Quantify uncertainty and manage data gaps through model input requirements and innovative methods
4. SSO4.- Increase the knowledge on climate related disasters (including interactions between compound events and cascading effects) by developing and implementing advanced modelling for multi-hazard assessment

This project has received funding from the European Union's Horizon Europe research and innovation programme under grant agreement No. 101093806. The publication reflects only the authors' views and the European Union is not liable for any use that may be made of the information contained therein.

5. SSO5.- Better assessment of holistic resilience and climate-related impacts for current and future scenarios
6. SSO6.- Better decision taking for cost-efficient adaptation solutions by developing a Decision Support System (DSS) to compare adaptation solutions
7. SSO7.- Ensure the use and impact of the ICARIA outputs

DRAFT

This project has received funding from the European Union's Horizon Europe research and innovation programme under grant agreement No. 101093806. The publication reflects only the authors' views and the European Union is not liable for any use that may be made of the information contained therein.

2. Objectives of deliverable

Across the three case study regions a variety of hazards, risk receptors and cascading effects are being considered (***Figure 1***). As part of Work Package 2 (WP2) "Modelling and multi-hazard assessment", the focus centres on the methodologies and tools used for the modelling of multi-hazard scenarios.

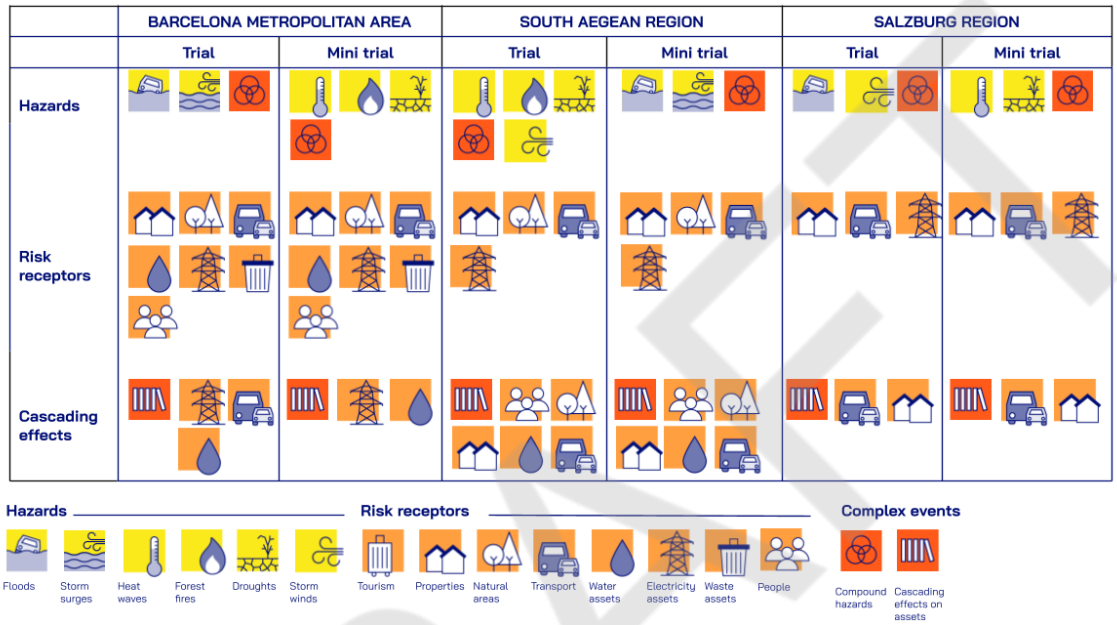

Figure 1. Summary of hazards and risk receptors considered in the different CS of ICARIA.

This deliverable, D2.4 "ICARIA Multi-Hazards Modelling Tools and Application Guidelines", is an updated version of D2.3 that documents the developments from Task 2.3, "Coupled Hazard Models: Methodology and Tools". Utilising the approaches outlined in previous tasks and deliverables within this WP a flexible modelling chain approach has been developed for the temporal and spatial coupling of different hazard combinations within the respective case studies.

The key objectives of this deliverable are thus summarised as the following:

- Provide a generalised framework for coupling of hazards and defining modelling chains for multi-hazard scenarios.
- Outline approaches for defining joint probability assessment of multi-hazard scenarios and means for selecting input parameters for multi-hazard modelling.
- Provide example guidelines for the spatial and temporal coupling multi-hazard models for:
    - Flooding (Pluvial) and Storm Surge,
    - Flooding and Extreme Wind,
    - Extreme Wind and Forest Fire,
    - Drought and Heatwave,
    - Drought and Forest Fire,
    - Heatwave and Forest Fire,

This project has received funding from the European Union's Horizon Europe research and innovation programme under grant agreement No. 101093806. The publication reflects only the authors' views and the European Union is not liable for any use that may be made of the information contained therein.

- Heatwave, Drought, and Forest Fire.

The framework outlined here provides a basis to produce compound hazard outputs that will subsequently be used within WP3 and WP4 to quantify the impact and its reduction caused by the adaptation solutions scenarios.

DRAFT

This project has received funding from the European Union's Horizon Europe research and innovation programme under grant agreement No. 101093806. The publication reflects only the authors' views and the European Union is not liable for any use that may be made of the information contained therein.

3. Generalised Compound Modelling Framework

For the modelling of multi-hazard scenarios, it is needed to consider events where different hazards have overlapping spatial extents and overlapping temporal extents (compound coincident hazards) or where the effects of one hazard may influence the magnitude and/or likelihood of subsequent hazards (compound consecutive hazards) within the same or part of the same region.

3.1 Physical Model Interactions

To facilitate the understanding of how different hazards can potentially interact with each other, their spatial and temporal extents should be defined. ***Figure 2*** from Gill and Malamud, (2014) outlines 16 different natural hazards and their respective spatial and temporal scales. The figure highlights how certain hazards may be both spatially and temporally isolated such as ground collapse, avalanche and local flash flooding whereas other hazards such as droughts that can last for prolonged duration and affect large areas. From the compound analysis assessment, this depiction facilitates understanding of directions of interactions such as hazard A occurring during hazard B and whether hazard A is likely to occur within the region of hazard B.

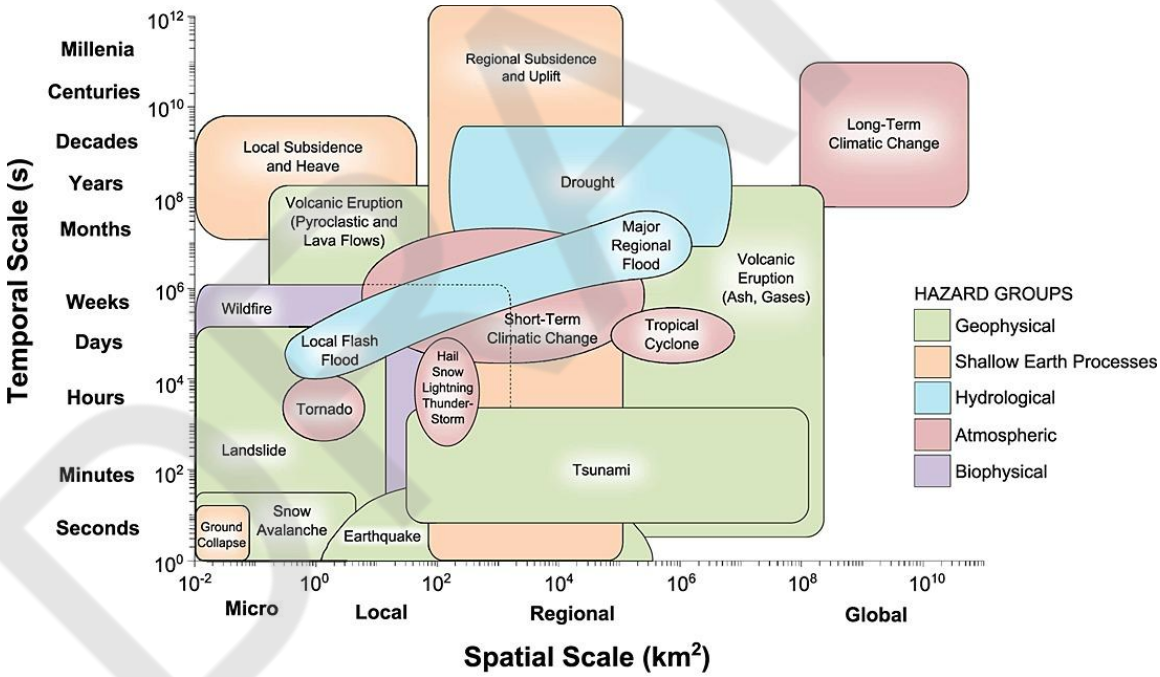

Figure 2. Spatial and temporal scales of 16 selected natural hazards, shown on logarithmic axes for spatial and temporal scales (Gill and Malamud, 2014).

Simplifying this depiction of spatial and temporal scales of hazards being modelled in ICARIA and referencing scales outlined in (Franzke, 2017) we identify the following scales (***Figure 3***).

This project has received funding from the European Union's Horizon Europe research and innovation programme under grant agreement No. 101093806. The publication reflects only the authors' views and the European Union is not liable for any use that may be made of the information contained therein.

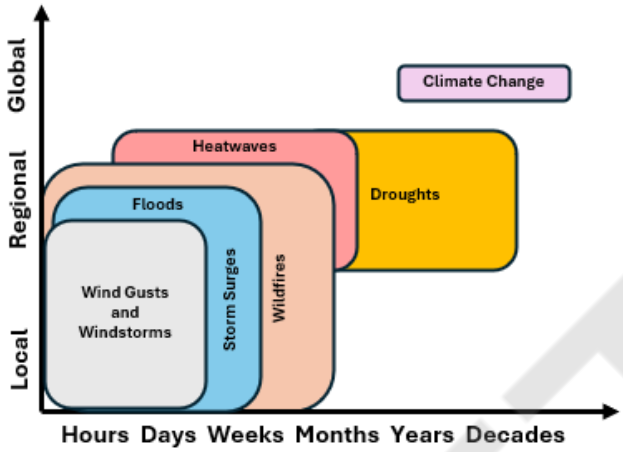

Figure 3. Spatial and temporal scales of modelled hazards within ICARIA (adapted from Franzke, 2017).

With spatial and temporal characteristics being considered for multi-hazard scenarios, consideration of cross hazard interactions is needed. These interactions include how the respective hazards interact with each other, how they relate to the vulnerability of the assets exposed to them, and any physical changes to the modelled extent via the hazards that could influence the behaviour of other modelled hazards. Hielkema et al, (2021) outlined four interaction pathways between two or more hazards that can be described as:

- ***Independent***: hazards affecting the same region either simultaneously or in sequence, where there is no triggering relationship or dependence between them.
- ***Triggering or Cascading***: The occurrence of one hazard results in the triggering of subsequent hazard/s. (e.g. earthquake triggering tsunami).
- ***Change conditions***: The environmental conditions within a region are altered due to a hazard occurring that in turn changes the likelihood of a subsequent hazard occurring. For instance drought changing conditions of vegetation within landscape which in turn alters the likelihood of wildfire ignition.
- ***Association***: Where two or more hazards are the result of the same triggering event. Such as an extreme rainfall event occurring in a region with sloped terrain leading to flooding and landslides.

To consider these aspects, a modelling chain can be plotted (***Figure 4***) whereby the time between Hazard 1 and Hazard 2 can range from 0 to *N* minutes/hours/days/months etc. depending on the interaction pathway of Hazard 1, its effects on the regions and assets with the region and the recovery time of affected assets and regional characteristics.

This project has received funding from the European Union's Horizon Europe research and innovation programme under grant agreement No. 101093806. The publication reflects only the authors' views and the European Union is not liable for any use that may be made of the information contained therein.

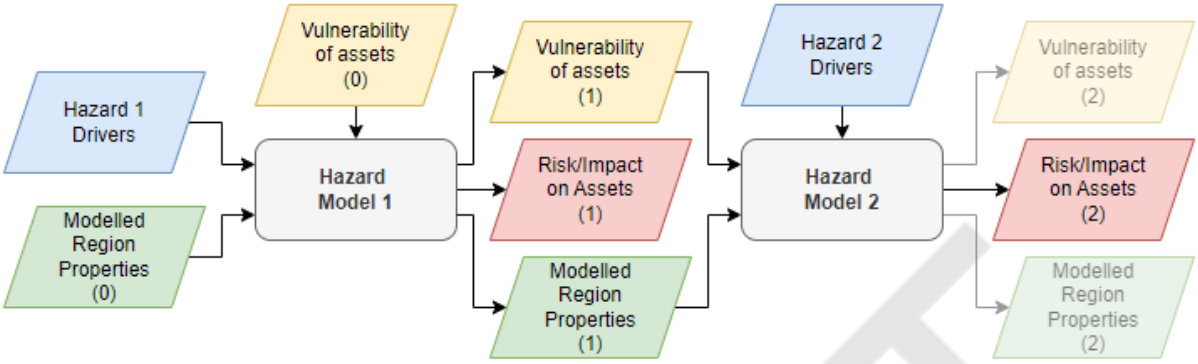

Figure 4. Physical interactions between hazards.

For the physical coupling of hazard models, Santiago-Collazo et al. (2019) outline 4 coupling approaches (***Table 1***). Within the multi-hazard modelling framework outlined within this deliverable, these 4 approaches are to be considered.

Table 1. Modelling approaches to coupling hazards (Santiago-Collazo et al., 2019).

Coupling technique	***Definition***
One-way	Computations that are transferred from one model and used as an input in another, often as boundary conditions
Loosely	Separately-running models are coupled using information exchange in an iterative manner
Tightly	Independent models are integrated into a single modelling framework by combining their source code
Fully	Governing equations of all the physical processes considered are solved simultaneously within the same modelling framework

This project has received funding from the European Union's Horizon Europe research and innovation programme under grant agreement No. 101093806. The publication reflects only the authors' views and the European Union is not liable for any use that may be made of the information contained therein.

3.1.1 Compound Coincident Hazards

Compound coincident hazards refer to two or more hazards that have both overlapping spatial extents and overlapping timeframes (***Figure 5***). For example, pluvial flooding occurring within the same coastal region being affected by flooding caused by a storm surge, or a wildfire occurring within a region currently experiencing drought would be defined as compound coincident hazards. Under such compound events the resulting impacts/risks are potentially greater than if they were to occur independently (Sutanto et al. 2020).

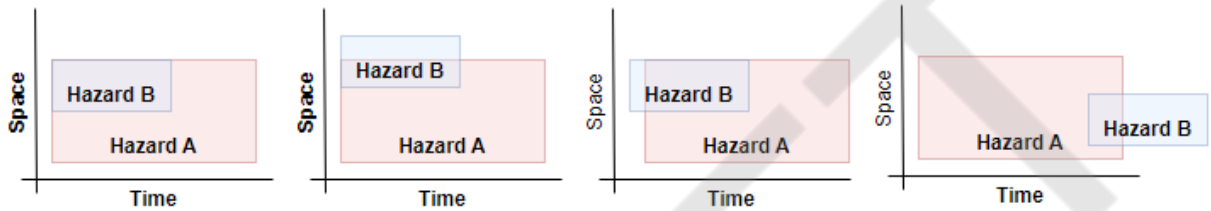

Figure 5. Compound Coincident Hazards.

3.1.2 Compound Consecutive Hazards

In contrast to compound coincident hazard events, whilst compound consecutive hazards have overlapping spatial extents, they are temporally separated, occurring in sequence (***Figure 6***).

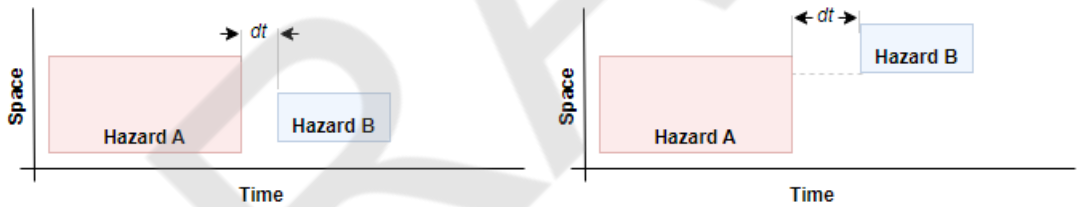

Figure 6. Compound Consecutive Hazards.

The occurrence of each hazard and time (dt) between them can influence the vulnerability of risk receptors in the region whilst also affecting the magnitude and probability of the following hazard occurring (de Ruiter et al., 2020). ***Figure 7*** from de Ruiter et al. (2020) depicts a timeline of consecutive hazards and how these influence the risk receptor (represented by the quality of the built environment) and their recovery times (ΔR). Within this example the rate of recovery of the built environment can vary and the subsequent shock of an additional hazard before the built environment has fully recovered can result in greater damage to the built environment.

This project has received funding from the European Union's Horizon Europe research and innovation programme under grant agreement No. 101093806. The publication reflects only the authors' views and the European Union is not liable for any use that may be made of the information contained therein.

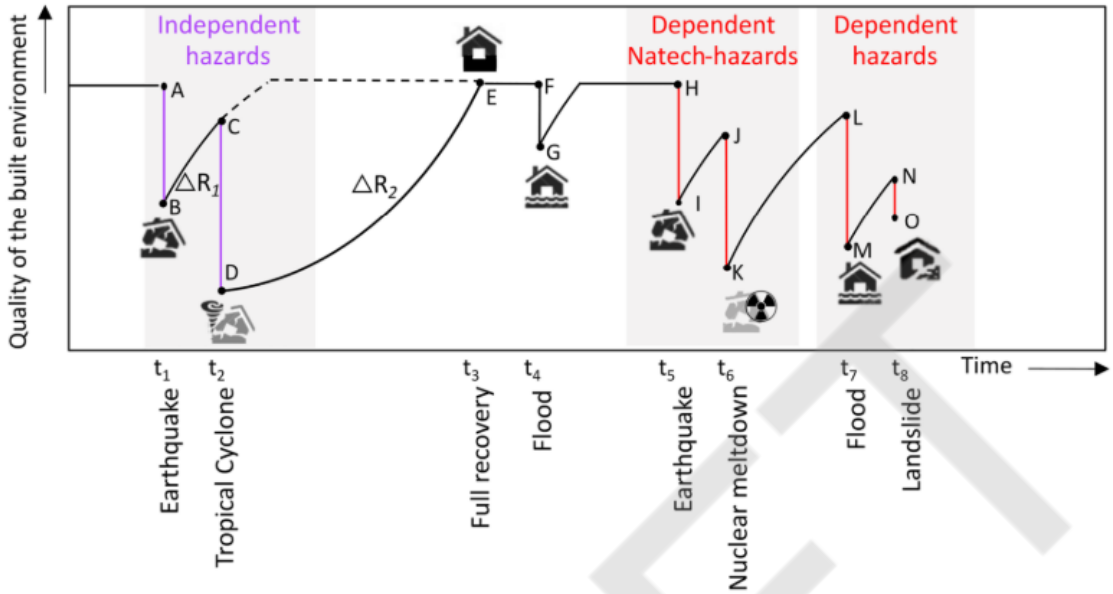

Figure 7. Schematic representation of consecutive disasters (de Ruiter et al., 2020).

These changes in the built environment and respective recovery rates are not limited solely to infrastructure but also to the environment itself as highlighted in Hielkema et al. (2021) relating to "change conditions" that can influence the magnitude and likelihood of proceeding events over time. Therefore, when modelling compound consecutive hazards considerable effort is needed for determining the characteristics of the environment and recovery of assets change over time post-event. Whilst recovery times of asset and services with respect to a range of hazards may be available from literature, and insurance data for example information as to the specifics relating to the recovery of a region may not be readily available and as such local knowledge through stakeholder engagement could serve as a valuable resource for determining recovery timeframes and parameters that need to be considered when modelling compound consecutive hazards.

3.2 Joint Probability Assessment

When defining the modelling parameters for joint probability assessment, it must be considered that for specified return periods there can exist a range of potential compound hazard values. The climate data used within the hazard modelling framework within ICARIA comes from the CMIP6 models that considers historical data from 1950 to 2014 and 4 Tier 1 SSPs (ssp126, ssp245, ssp370 and ssp585) ranging from 01/01/2015 to 31/12/2100). The selected CMIP6 models being utilised within the hazard assessments are outlined in ***Table 2*** with further details relating to the approaches used for downscaling and statistical analysis available in D1.2. "Climate Projections and Hazard Scenarios" (ICARIA 2023a).

With this range of models and SPPs being considered there is a need to adopt an approach to consider the various likelihoods and magnitudes of climate input data that will be generated for use within the hazard models and the subsequent uncertainties. To address these considerations from the hazard driver perspective, the proposed joint probability assessment within ICARIA is defined over 4 steps:

This project has received funding from the European Union's Horizon Europe research and innovation programme under grant agreement No. 101093806. The publication reflects only the authors' views and the European Union is not liable for any use that may be made of the information contained therein.

1. Consider all scenarios (40 statistical and 8 dynamical) for each climate variable produced that will be applied within the respective compound hazard models.
2. Within each hazard model, select the SSPs for each variable and define the joint probability of compound events.
3. Based on steps 1 and 2, 48 joint probability distributions are available for each time period considered.
4. Sort all these probabilities by probability of occurrence so that, for each compound event, it is possible to select scenarios for modelling that correspond to the median (most likely) and 90th Percentile (for uncertainty assessment).

Table 2. Information about the 10 climate models belonging to the 6 Coupled Model Intercomparison Project (CMIP6) corresponding to the IPCC AR6. Models were retrieved from the Earth System Grid Federation (ESGF) portal in support of the Program for Climate Model Diagnosis and Intercomparison (PCMDI) (Deliverable 1.2).

CMIP6 MODELS	Resolution	Responsible Centre	References
ACCESS-CM2	1,875º x 1,250º	Australian Community Climate and Earth System Simulator (ACCESS), Australia	Bi et al (2020)
BCC-CSM2-MR	1,125º x 1,121º	Beijing Climate Center (BCC), China Meteorological Administration, China.	Wu et al. (2019)
CanESM5	2,812º x 2,790º	Canadian Centre for Climate Modeling and Analysis (CC-CMA), Canadá.	Swart et al. (2019)
CMCC-ESM2	1,000º x 1,000º	Centro Mediterraneo sui Cambiamenti Climatici (CMCC).	Cherchi et al. (2018)
CNRM-ESM2-1	1,406º x 1,401º	CNRM (Centre National de Recherches Meteorologiques), Meteo-France, Francia.	Seferian (2019)
EC-EARTH3	0,703º x 0,702º	EC-EARTH Consortium	EC-Earth Consortium (2019)
MPI-ESM1-2-HR	0,938º x 0,935º	Max-Planck Institute for Meteorology (MPI-M), Germany.	Müller et al. (2018)
MRI-ESM2-0	1,125º x 1,121º	Meteorological Research Institute (MRI), Japan.	Yukimoto et al. (2019)
NorESM2-MM	1,250º x 0,942º	Norwegian Climate Centre (NCC), Norway.	Bentsen et al. (2019)
UKESM1-0-LL	1,875º x 1,250º	UK Met Office, Hadley Centre, United Kingdom	Good et al. (2019)

This project has received funding from the European Union's Horizon Europe research and innovation programme under grant agreement No. 101093806. The publication reflects only the authors' views and the European Union is not liable for any use that may be made of the information contained therein.

For compound coincident hazards, if they share common drivers, the probability of extremes affecting the same regions within the same timeframe may have some dependencies. For example, the climate conditions associated with a heatwave may also influence the magnitude of the Fire Weather Index (FWI) score (***Figure 8***a), or the climate drivers relating to a Storm Surge (SS) may also influence the magnitude and likelihood of heavy rainfall within the same region (***Figure 8***b) within their respective timeframes.

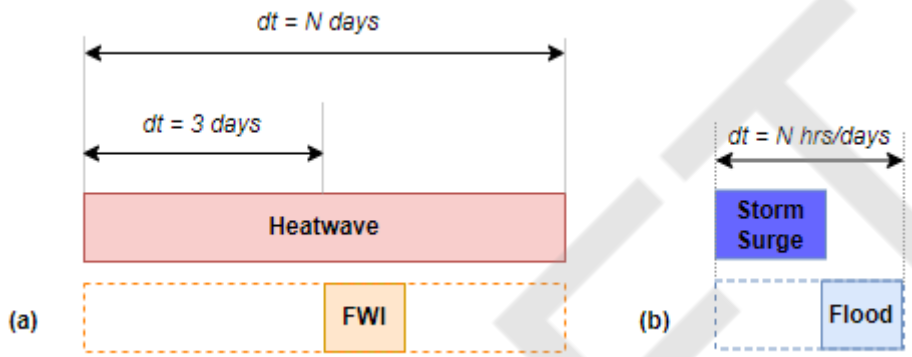

Figure 8. Temporal depiction of compound coincident hazards at different time scale ranges.

It is possible to visualise the relationship between different hazard drivers via plotting them together within a bivariate plot. ***Figure 9*** shows variation in maximum daily rainfall vs maximum wind speed values and their respective marginal distributions) taken from baseline historical records between 1981 and 2010 f Salzburg case study. The figure shows wide variations in wave heights at low rainfall values (≤5mm/day). The historical data shows a limited number of recorded days where daily recorded rainfall is > 5mm with low maximum wave height values on these days.

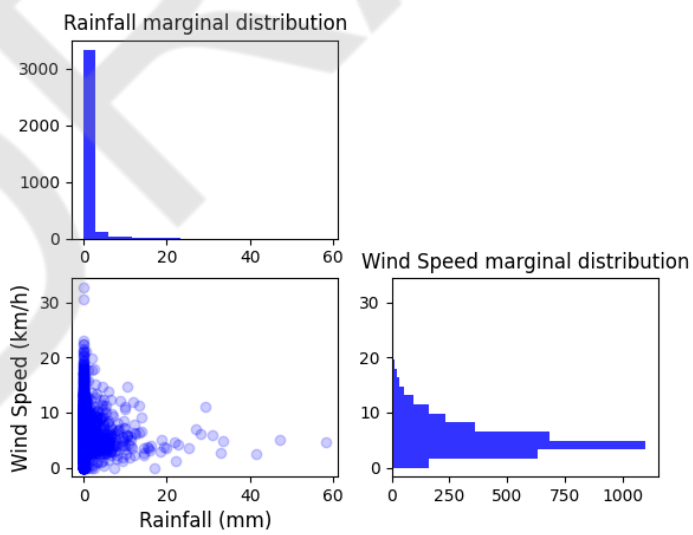

Figure 9. Marginal distribution of daily rainfall and maximum wind speed for Salzburg baseline case (*Historical Data*).

This project has received funding from the European Union's Horizon Europe research and innovation programme under grant agreement No. 101093806. The publication reflects only the authors' views and the European Union is not liable for any use that may be made of the information contained therein.

With the data being utilised to assess Joint Probability being at daily resolution, the probability of Hazard 1 occurring at same time, or within a specified timeframe of Hazard 2, would also be in terms of days. As such, to approximate return periods (RPs), it is necessary to convert from daily to annual probabilities. Once P (occurring in a day) is calculated, it is possible to follow the following 3 steps to convert to annual probabilities:

1. Determine probability of event not occurring on a single day

$$P(not\ occuring\ in\ a\ day) = 1 - P(occuring\ in\ a\ day)$$

2. Probability of event not occurring on any day within a year

$$P(not\ occuring\ in\ a\ year) = P(not\ occurring\ in\ a\ day)^{365.25}$$

3. Probability of occurring at least once in a year

$$P(occurring\ at\ least\ once\ per\ year) = 1 - P(not\ occuring\ in\ a\ year)$$

Nevertheless, there are multiple combinations of hazards attributes with the same daily Joint Probability such that a further methodology was developed to evaluate the relationships between bivariate data, Copulas that join/couples multivariate data together can be used.

3.2.1 Bivariate Copula Assessment

Copulas refer to a mathematical approach for modelling the dependence between two or more random variables (Schmidt 2006). Within the scope of multi-hazard modelling they have been used to define the joint probabilities of a range of hazard combinations including heatwaves and droughts (Ballarin et al., 2021, Páscoa et al. 2024), extreme wind and flooding (Bloomfield. et al., 2023), and Pluvial, Fluvial, and Storm Surge flooding (Ming et al., 2022). The Copulae library within Python (Bok, 2025) was applied to map the historical data to a copula and utilise this data to derive synthetic data based on the underlying correlation of the original dataset if present. ***Figure 10*** shows synthetic data consisting of 10 times of data points derived from the historical data via the use of a Clayton copula.

The synthetic data were compared to the original historical data, shown in ***Figure 11***, to ensure that derived datasets have maintained the same probabilistic distribution to the original datasets.

This project has received funding from the European Union's Horizon Europe research and innovation programme under grant agreement No. 101093806. The publication reflects only the authors' views and the European Union is not liable for any use that may be made of the information contained therein.

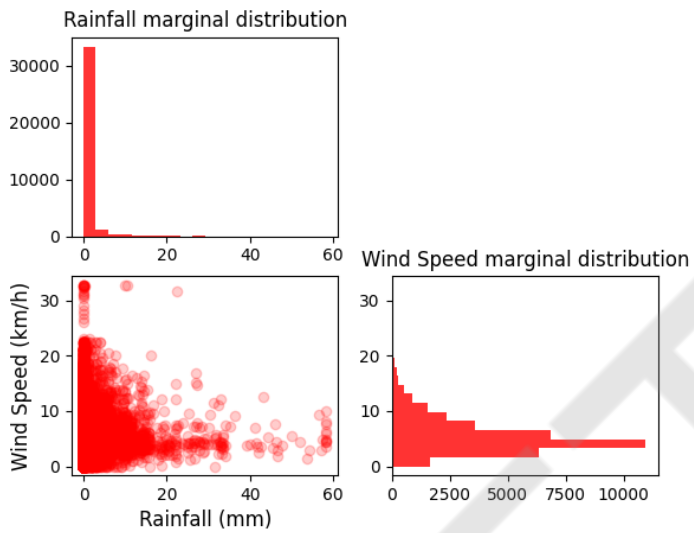

Figure 10. Marginal distribution of daily rainfall and maximum wind speed for Salzburg baseline case (*Synthetic Data*).

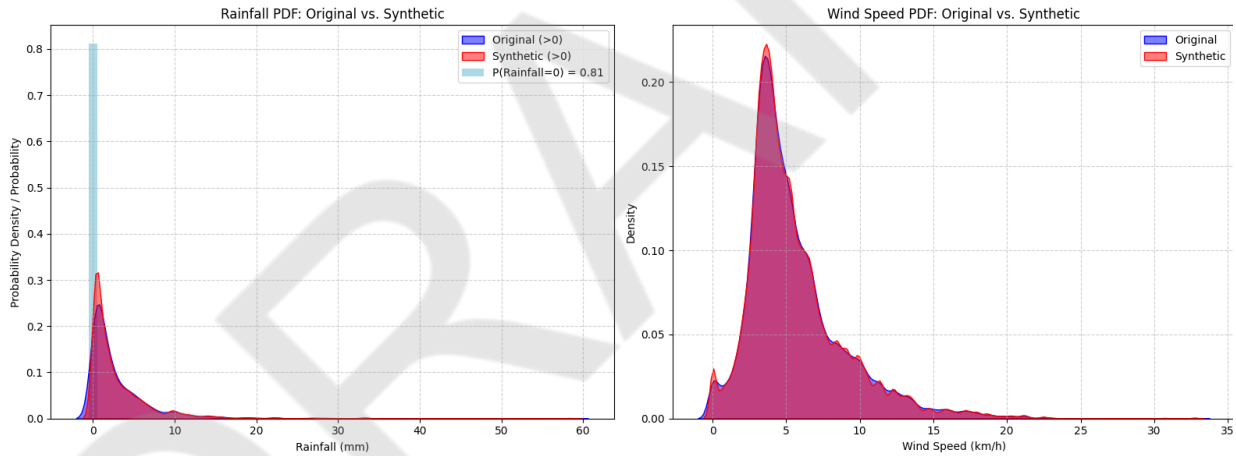

(a) (b)

Figure 11. The comparisons of the probability distribution functions of Daily rainfall (left) and Maximum wind speed (right).

Although the joint probability can also be estimated statistically from the historical and synthetic data, it will require specifying the thresholds of hazards such that the occurrence of events exceeding the thresholds could be determined. However, this approach can only produce information related to given combinations of hazard values that do not provide all possible combinations of hazard attributes. Thus, an alternative approach was developed. Through the Coupla analysis, a grid covering the dataspace was developed to describe the daily joint probability of the two hazard variables, which was further converted into contours of annual joint probability. The point data in ***Figure 12*** show the daily joint probability for the combinations of daily rainfall and maximum wind speed for historical (left) and synthetic (right) data, while the contours show the annual joint probability. ***Figure 12*** enables identifying all combinations of daily rainfall and maximum wind speed that have the equivalent annual

This project has received funding from the European Union's Horizon Europe research and innovation programme under grant agreement No. 101093806. The publication reflects only the authors' views and the European Union is not liable for any use that may be made of the information contained therein.

joint probability in order to evaluate their consequences. For the analysis of compound coincident events, firstly a leading hazard and then a secondary hazard that occurs within a given timeframe should be identified. Compound consecutive events can relate to different hazards (***Figure 13***a) and the same hazard type occurring in succession (***Figure 13***b).

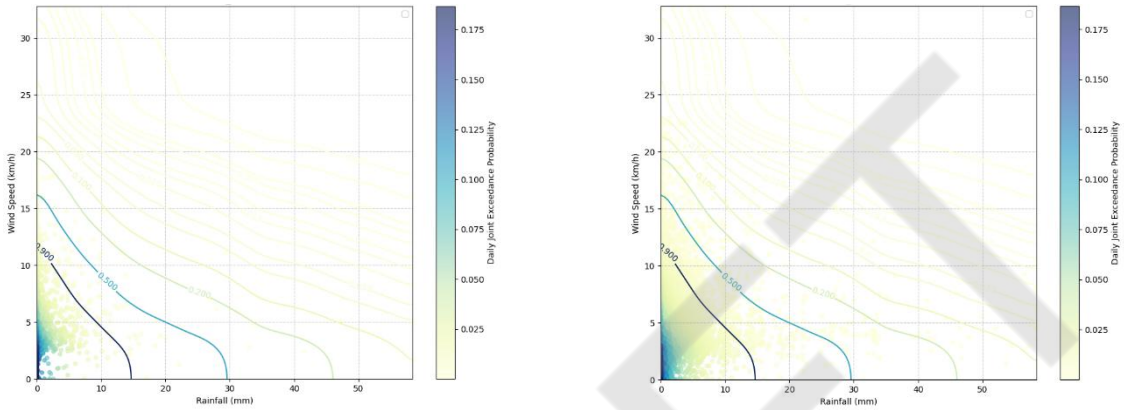

(a) (b)

Figure 12. Daily joint probability of daily rainfall and maximum wind speed combinations (points), and the derived annual joint probability contours for the (a) historical and (b) synthetic data under the baseline scenario.

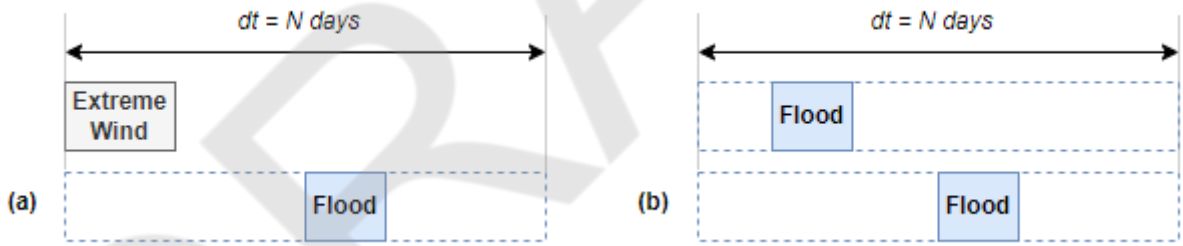

Figure 13. Temporal depiction of compound consecutive hazards.

To model these kinds of compound events we thus need to determine the limits for temporal duration (*N*) between events whereby the influence/effects of Hazard 1 still affect the effects of Hazard 2 within the modelled region. To plot this data a time window of duration *N* can be specified, and for each recorded value of hazard 1 (e.g. rainfall) the maximum value of hazard 2 (e.g. maximum Wind Speed) that occurs within *N* days of hazard 1 is recorded. ***Figure 14*** shows a comparison between probability distributions of wind gust speed and rainfall of Salzburg in 2071-2099 under SSP126 and SSP585 scenarios for (a) compound events, (b) consecutive events within a 7-day time window, and (c) consecutive events within a 30-day time window. The examples show that the enlarged time window leads to higher chances for the combinations of intense daily rainfall and strong maximum wind speed such that both daily and annual joint probability have increased. The larger the time window is, the greater joint probability is.

This project has received funding from the European Union's Horizon Europe research and innovation programme under grant agreement No. 101093806. The publication reflects only the authors' views and the European Union is not liable for any use that may be made of the information contained therein.

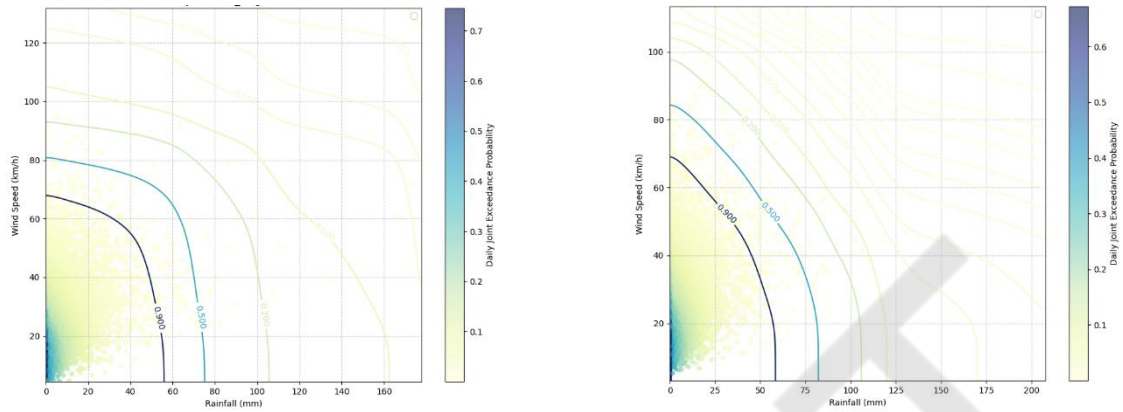

(a)

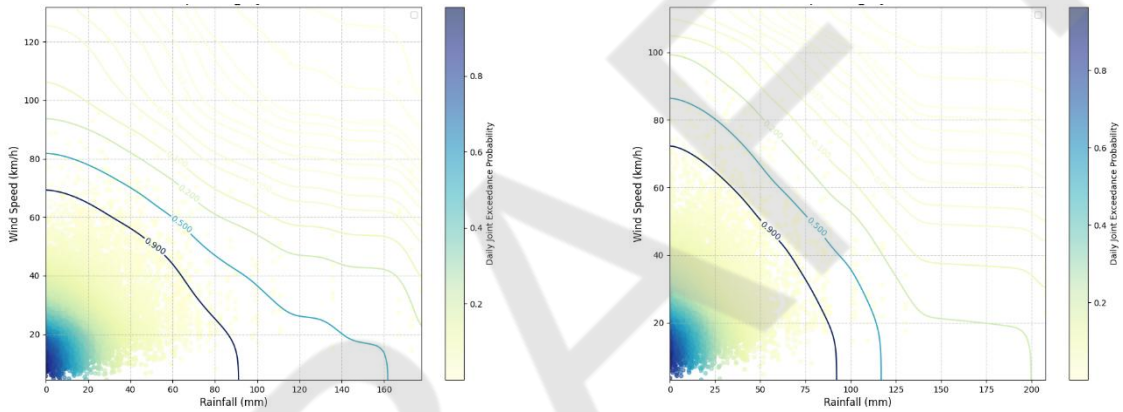

(b)

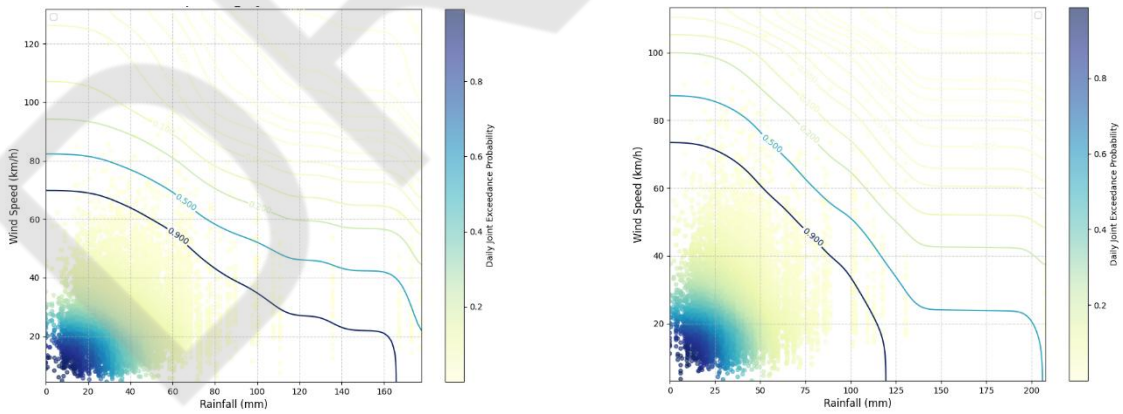

(c)

Figure 14. Daily joint probability of daily rainfall and maximum wind speed combinations (points), and the annual joint probability (contours) for 2071-2099 period under SSP 126 (left) and SSP 585 (right) scenarios for (a) compound events, (b) consecutive events within a 7-day time window (c) consecutive events within a 30-day time window.

This project has received funding from the European Union's Horizon Europe research and innovation programme under grant agreement No. 101093806. The publication reflects only the authors' views and the European Union is not liable for any use that may be made of the information contained therein.

As outlined at the beginning of this section, the ICARIA project employs a variety of climate models, each coupled with several SSPs. Due to differences within these climate models, a range of distinct joint probability distributions are generated. ***Figure 15*** presents a comparison of the joint probability distributions between the EC-EARTH3 model and the CanESM5 model. This comparison reveals a higher probability of increased daily rainfall events in the CanESM5 model compared to the EC-EARTH3 model. To consider these differences between the respective climate models, the derived joint probability hazard input values for modelled return periods will be considered from each model with the median and 90th percentile values being utilised. To account for the differences between the respective climate models, the derived joint probability distributions will be analysed for each model for selected return periods. Both the median and 90th percentile values from these results could then be utilised as input parameters for the physical modelling.

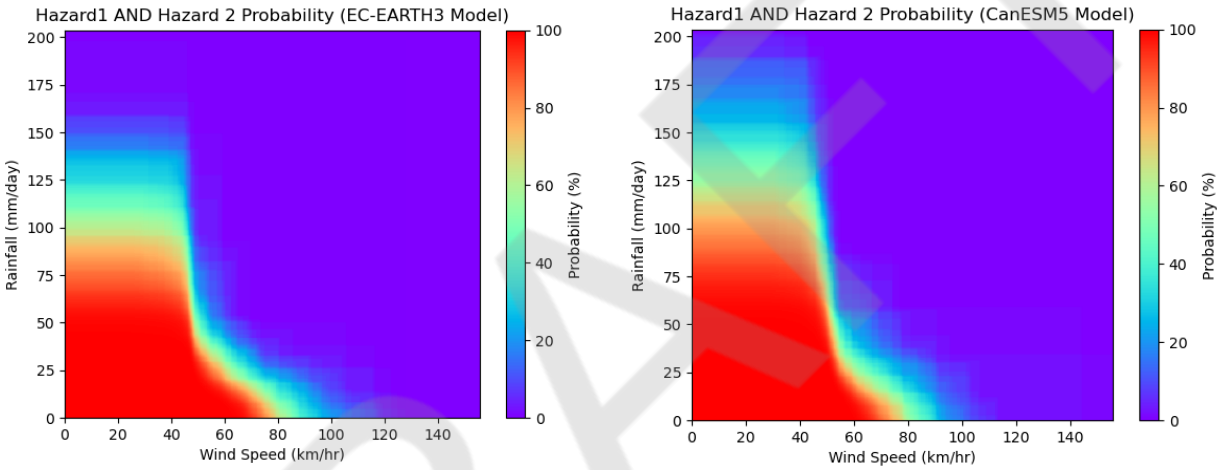

(a) (b)

Figure 15. Combined Joint Probability of SSPs 126, 245, 370, and 585 for (a) EC-EARTH3 climate model and (b) CanESM5 climate model.

Through analysis of compound wind and rainfall events across 4 SSPs (126, 245, 370, and 585), multiple downscaled models were analysed. For the wind speed, each SSP included 6 statistical downscaled models (ACCESS-CM2, CanESM5, CMCC-ESM2, CNRM-ESM2-1, EC-EARTH3, and MRI-ESM2-0) that were analysed to derive the events with different return periods (***Figure 16***). For daily rainfall data, 10 downscaled models (MPI-ESM1-2-HR, BCC-CSM2-MR, CanESM5, CMCC-ESM2, EC-EARTH3, NorESM2-MM, ACCESS-CM2, CNRM-ESM2-1, MRI-ESM2-0, and UKESM1-0-LL) were analysed to estimate the events with different return periods (***Figure 17***).

This project has received funding from the European Union's Horizon Europe research and innovation programme under grant agreement No. 101093806. The publication reflects only the authors' views and the European Union is not liable for any use that may be made of the information contained therein.

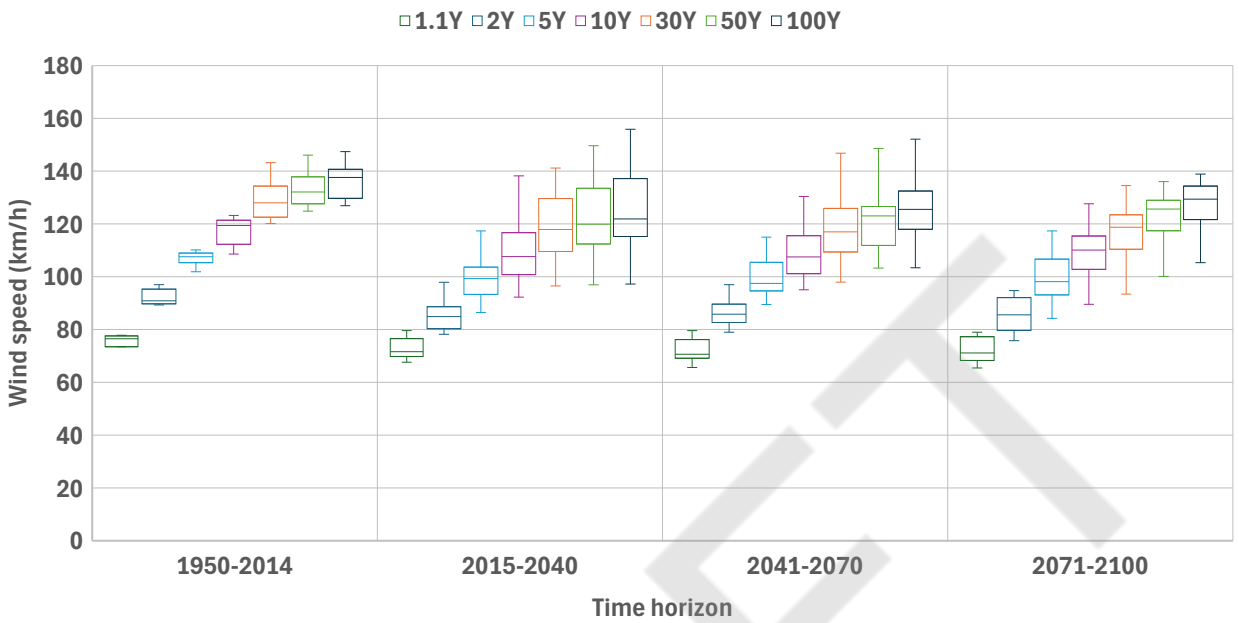

Figure 16. Maximum wind speed for 1.1, 2, 5, 10, 30, 50, and 100 year return periods using 4 SSPs (126, 245, 370, and 585), each includes 6 climate models (ACCESS-CM2, CanESM5, CMCC-ESM2, CNRM-ESM2-1, EC-EARTH3, and MRI-ESM2-0).

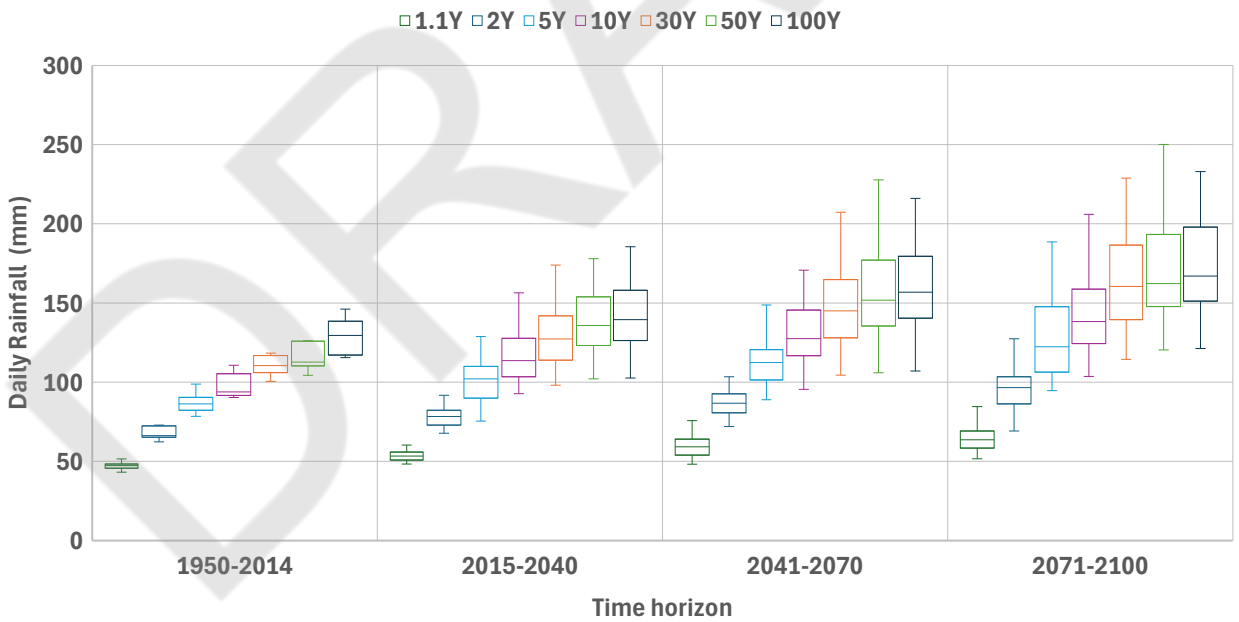

Figure 17. Daily rainfall for 1.1, 2, 5, 10, 30, 50, and 100 year return periods using 4 SSPs (126, 245, 370, and 585), each includes 10 climate models (MPI-ESM1-2-HR, BCC-CSM2-MR, CanESM5, CMCC-ESM2, EC-EARTH3, NorESM2-MM, ACCESS-CM2, CNRM-ESM2-1, MRI-ESM2-0, and UKESM1-0-LL).

This project has received funding from the European Union's Horizon Europe research and innovation programme under grant agreement No. 101093806. The publication reflects only the authors' views and the European Union is not liable for any use that may be made of the information contained therein.

Here the joint probability values were derived for each model and their respective SSPs resulting in 24 (wind speed) and 30 (rainfall) joint probability distributions. Based on these distributions box plots were generated for six annual return periods (1.1, 2, 5, 10, 30, 100). The results highlight that whilst the upper ranges of maximum wind speed and rainfall values increase with more severe events the median rainfall value decreases highlighting the observation from ***Figure 14***a that heavier rainfall events are less likely to occur at higher maximum Wind Speeds. Though using this approach median and 90th percentile values for each return period can be derived (**¡Error! La autoreferencia al marcador no es válida.** and ***Table 4*** for wind speed; ***Table 5*** and ***Table 6*** for daily rainfall) for use within the compound model setup to analyse the most likely compound hazard scenario for a given return period and uncertainty that considers potential extremes for this return period. The results show that the uncertainty pf projections in wind speed during 2015-2040 time horizon will be larger than other time horizons with greater extremes, but the mean values in the future projections are lower the one in the historical period 1950-2014. For daily rainfall, both the magnitude and uncertainty will increase more significantly into far futures.

DRAFT

This project has received funding from the European Union's Horizon Europe research and innovation programme under grant agreement No. 101093806. The publication reflects only the authors' views and the European Union is not liable for any use that may be made of the information contained therein.

Table 3. The median estimation of 1.1, 2, 5, 10, 30 and 100 year return period wind gust within SLZ region derived from 4 SSPs (126, 245, 370, and 585), each includes 6 climate models (ACCESS-CM2, CanESM5, CMCC-ESM2, CNRM-ESM2-1, EC-EARTH3, and MRI-ESM2-0).

Return Period (Years)	***Wind Speed (km/hr)***			
	1950-2014	***2015-2040***	***2041-2070***	***2071-2100***
1.1	76.5	71.6	70.7	71.1
2	90.9	84.9	85.8	85.6
5	107.6	99.3	97.5	98.1
10	119.4	107.6	107.5	110.1
30	128.0	117.9	117.0	118.8
50	132.1	119.9	123.0	125.6
100	137.6	121.9	125.5	129.4

Table 4. The 90th percentile estimation of 1.1, 2, 5, 10, 30 and 100 year return period wind gust within SLZ region derived from 4 SSPs (126, 245, 370, and 585), each includes 6 climate models (ACCESS-CM2, CanESM5, CMCC-ESM2, CNRM-ESM2-1, EC-EARTH3, and MRI-ESM2-0).

Return Period (Years)	***90th percentile Wind Speed (km/hr)***			
	1950-2014	***2015-2040***	***2041-2070***	***2071-2100***
1.1	77.7	78.4	78.8	78.5
2	95.8	93.7	93.4	93.2
5	109.4	110.6	107.1	108.2
10	122.0	120.3	120.1	116.8
30	137.3	135.3	132.6	131.5
50	140.6	143.0	135.2	133.1
100	142.9	147.3	136.9	138.1

DRAFT

This project has received funding from the European Union's Horizon Europe research and innovation programme under grant agreement No. 101093806. The publication reflects only the authors' views and the European Union is not liable for any use that may be made of the information contained therein.

Table 5. The median estimation of 1.1, 2, 5, 10, 30 and 100 year return period wind gust within SLZ region derived from 4 SSPs (126, 245, 370, and 585), each includes 10 climate models (MPI-ESM1-2-HR, BCC-CSM2-MR, CanESM5, CMCC-ESM2, EC-EARTH3, NorESM2-MM, ACCESS-CM2, CNRM-ESM2-1, MRI-ESM2-0, and UKESM1-0-LL).

Return Period (Years)	Daily Rainfall (mm)			
	1950-2014	2015-2040	2041-2070	2071-2100
1.1	47.3	53.3	59.2	63.6
2	66.3	78.3	86.7	96.6
5	86.3	102.1	112.4	122.3
10	93.9	113.5	127.5	138.3
30	110.5	127.3	145.0	160.5
50	112.7	135.7	151.8	162.3
100	129.5	139.5	156.8	166.9

Table 6. The 90th percentile estimation of 1.1, 2, 5, 10, 30 and 100 year return period wind gust within SLZ region derived from 4 SSPs (126, 245, 370, and 585), each includes 10 climate models (MPI-ESM1-2-HR, BCC-CSM2-MR, CanESM5, CMCC-ESM2, EC-EARTH3, NorESM2-MM, ACCESS-CM2, CNRM-ESM2-1, MRI-ESM2-0, and UKESM1-0-LL).

Return Period (Years)	Daily Rainfall (mm)			
	1950-2014	2015-2040	2041-2070	2071-2100
1.1	48.9	58.5	65.7	73.2
2	72.6	85.5	98.2	115.2
5	93.9	117.3	128.0	167.8
10	110.7	136.5	157.8	194.9
30	121.4	158.3	186.7	213.7
50	130.0	166.7	198.8	218.2
100	148.9	180.9	209.9	219.4

This project has received funding from the European Union's Horizon Europe research and innovation programme under grant agreement No. 101093806. The publication reflects only the authors' views and the European Union is not liable for any use that may be made of the information contained therein.

3.2.2 Bivariate Copula Assessment with Linear Regression

For the analysis in South Aegean Region, the simple application of bivariate Copula is unable to describe the relationship between the maximum wind speed and the FWI adequately. ***Figure 18*** shows the marginal distribution of the maximum wind speed and the FWI for (a) the historical data and (b) the synthetic data created by using Copula method only. There is a clear polynomial linear relationship, which will be further explained in Section 5.3.1, for the upper bound values of FWI and the maximum wind speed in ***Figure 18***a that is not reflected in the synthetic data in ***Figure 18***b. Thus, the polynomial linear regression was further combined with the bivariate Copula analysis to derive the relationship between the two variables. The result obtained, shown in ***Figure 19***, has capture the relationship between the upper bound of FWI and the maximum Wind Speed.

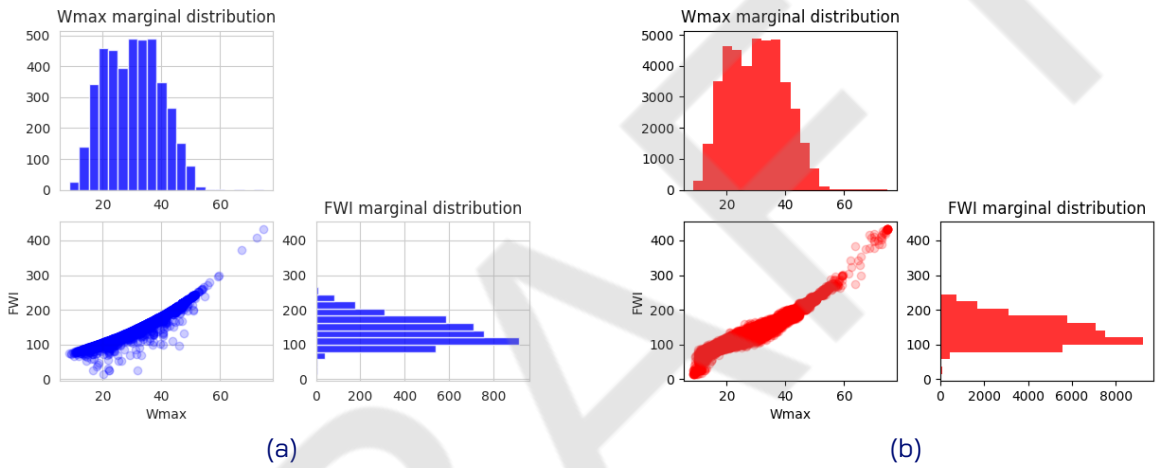

Figure 18. Marginal distribution of maximum wind speed and FWI for KOS in South Aegean Region (KOS) baseline (a) historical data (b) Synthetic data with bivariate Copula only.

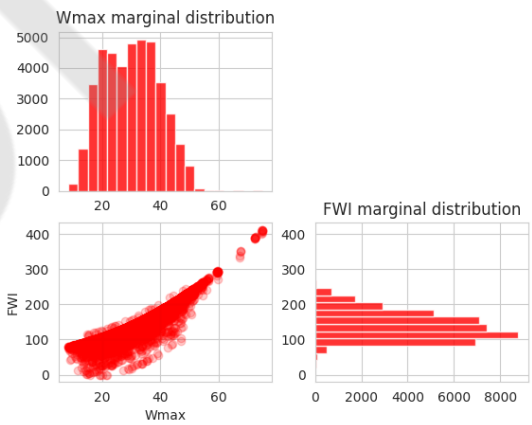

Figure 19. Marginal distribution of maximum wind speed and FWI for South Aegean Region (KOS) baseline case (Synthetic data with bivariate Copula and linear regression).

This project has received funding from the European Union's Horizon Europe research and innovation programme under grant agreement No. 101093806. The publication reflects only the authors' views and the European Union is not liable for any use that may be made of the information contained therein.

3.2.3 Multivariate Copula Assessment

The multivariate Copula assessment was applied to analyse the relationship between the three variables Maximum Temperature, Maximum wind speed and FWI for the South Aegean Region. As a results, an interactive user interface was created to allow the inspection of the data relationships in a 3D manner, as shown in ***Figure 20***. However, for Multivariate Copula analysis, there is only Gaussian Distribution could be applied such that this will not be able to describe the polynomial linear relationship between the maximum wind speed and FWI. The comparison between of the historical data (***Figure 20***a) and the synthetic data (***Figure 20***b) demonstrates significant difference in the cumulative distribution functions of both datasets. Using the bivariate Copula or bivariate Copula with Linear Regression could simply the complexity and better describe the relationship among the variables.

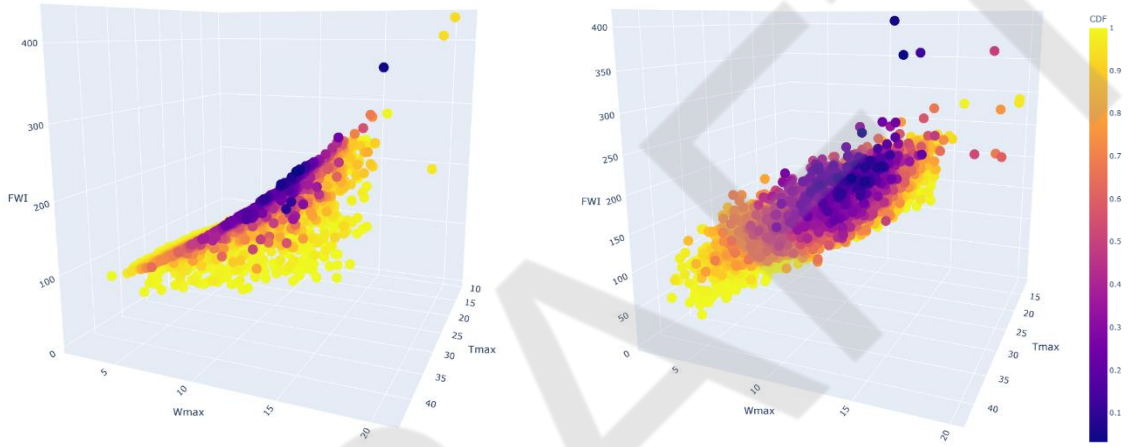

(a) (b)

Figure 20. Multivariate Copula Analysis of maximum temperature, maximum wind speed and FWI for KOS in the South Agena Region (a) historical data (b) synthetic data.

This project has received funding from the European Union's Horizon Europe research and innovation programme under grant agreement No. 101093806. The publication reflects only the authors' views and the European Union is not liable for any use that may be made of the information contained therein.

4. Single Hazard Models Overview

The multi-hazard scenarios being considered within the ICARIA across the three case studies are derived from combinations of six different climate driven hazard types (***Figure 21***), with different combinations of hazards being selected by respective case studies.

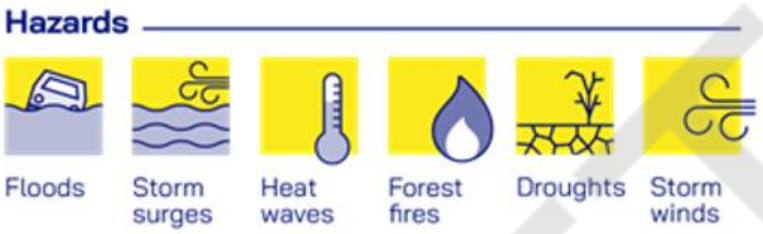

Figure 21. Hazard Classifications being modelled within ICARIA.

As an initial basis for selecting scenarios to be modelled as part of the multi-hazard assessment, it was defined what are the hazard drivers used within the hazard model and how extreme events are defined from a single hazard perspective (***Table 7***). This information will later be used to facilitate the derivation of joint probabilities of compound events and for the selection of multi-hazard scenarios that will be modelled.

Table 7. Extreme event definitions for modelled hazards.

Hazard Model	*Hazard Drivers*	*Extreme Event Definition*
Pluvial flood	Precipitation	Heavy to extreme rainfall days range from 20 mm/day to 100 mm/day. IDF curves used to simulate RPs of 2,10 and 100 years.
Storm surge	Significant Wave Height and Tide levels	90th percentile
Storm winds	Windspeed	Hazardous wind speeds > 70 km/hr are being considered
Drought	Precipitation	Standardised Precipitation Index (SPI) where: -1.00⩾SPI>-1.50: moderate drought -1.50⩾SPI>-2.00: severe drought -2.00⩾SPI: extreme drought
Heatwave	Temperature	95th percentile of summer months for 3 or more days
Forest Fire	Temperature, Windspeed, Precipitation, Relative humidity	FWI where >= 70 would represent extreme fire danger ISI where >=13.4 windspeed >= 40km/hr

This project has received funding from the European Union's Horizon Europe research and innovation programme under grant agreement No. 101093806. The publication reflects only the authors' views and the European Union is not liable for any use that may be made of the information contained therein.

5. Model Setup Guidelines

5.1 Flooding (Pluvial) and Storm Surge

5.1.1 Compound Model setup

The occurrence of a compound event of storm surge and pluvial flooding generates challenging flood management scenarios in coastal areas due to the interactions established between both hazards. On the one hand, a storm surge entails a temporary rise of the mean sea level and maximum wave height. On the other hand, in an urban area, during rain events, the amount of water running through the sewer network increases due to the large volume of runoff generated, stressing drainage infrastructures.

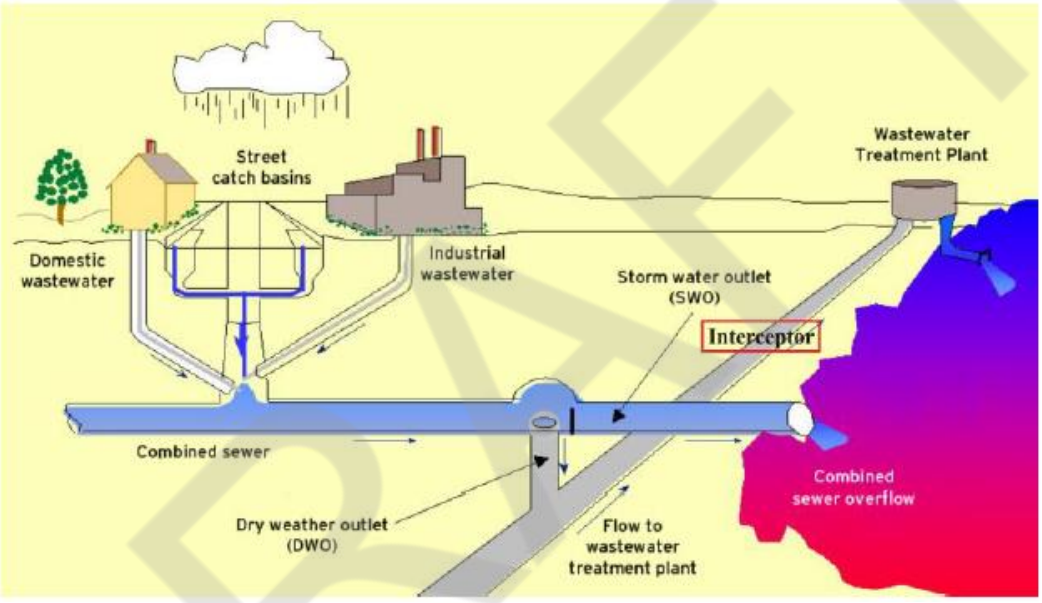

Figure 22. Scheme of a sewer system and the sewer interceptor.

In case of combined sewer systems, under dry water conditions, the wastewater generated in a city is conveyed to the local wastewater treatment plant through sewer pipes. However, rain events above certain return periods, usually involving high rain intensities in short time periods, can generate a water flow above their maximum capacity. In these situations, the exceeding water is directly discharged from the surcharged pipes to the water receiving body (without previous treatment) through outfalls. In case of combined sewer systems, this phenomenon is known as combined systems overflow (CSO). In coastal areas, the receiving water body is often the sea. Outfalls that discharge water on the sea during CSOs are built at the shoreline considering a safety height above the mean sea level to prevent sea water entering the drainage network.

However, during storm surge events, the mean sea level can rise to the point where this safety height is exceeded by a transitory extreme sea level. If this occurs, sea water is able to intrude the outlet of the urban drainage systems though the lowermost point of the outfall pipes. As a result, the drainage capacity of the whole network is reduced according to the degree of seawater intrusion. This situation, which corresponds to a backwater phenomenon, can lead to upstream saturation of the drainage

This project has received funding from the European Union's Horizon Europe research and innovation programme under grant agreement No. 101093806. The publication reflects only the authors' views and the European Union is not liable for any use that may be made of the information contained therein.

network leading to flooding in upstream parts of the network drainage area (***Figure 23***) (Ming et al., 2022; Laster Grip et al., 2021; Bevacqua et al. 2019; Qiang et al., 2021a, Domingo et al., 2010).

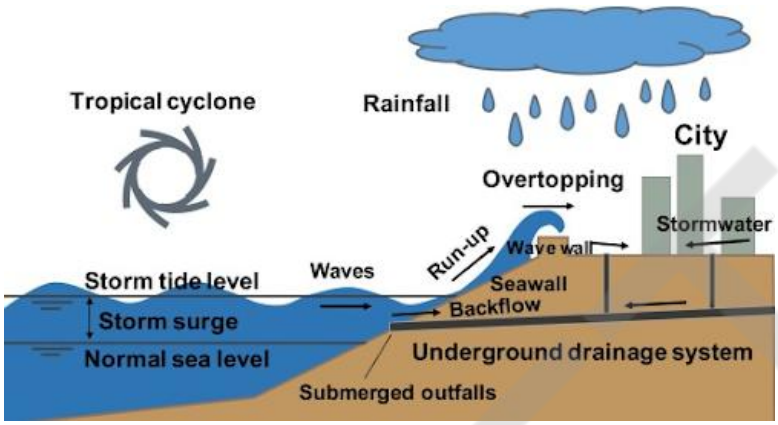

Figure 23. Conceptual model of the occurrence of backwater effect (Qiang et al., 2021a).

Furthermore, this kind of compound events have an important parallel effect on coastal low-lying areas. A temporary sea level rise can lead to the intrusion of seawater as overland flow in low gradient terrain which are unprotected to this phenomenon. Just by itself, this can cause important floods. In combination with extreme precipitation, where extensive runoff circulates on the surface, the dynamics established between both floods can lead to more extensive flooded areas in the mentioned terrain (Santiago-Collazo et al., 2019).

Deliverable 2.1 of project ICARIA (Crisi-Adapt II 2020) presented a series of methodologies to develop hazard assessments of the different single hazard scenarios considered in the three case studies.

- Modelling of pluvial flooding with 1D/2D hydrodynamic model based on solving the free complete flow equations (mass and momentum equations), where the 1D and the 2D domains correspond to the sewer network and the urban surface respectively.
- Assessment of temporary extreme sea level with an hydrostatic model based on tides and wave height observations.

As mentioned earlier, the sewer network outfalls discharging water directly on the sea are the key structural element where pluvial water/wastewater and seawater interact during compound events. They are the entry points where seawater can intrude the sewer network, reducing surface drainage capacity and even leading to the direct flooding of coastal low-lying urban areas through inlets and manholes.

Despite being a well acknowledged problematic (Azevedo de Almeida et al., 2016; Meyers et al., 2021; Qiang et al., 2021; Kim et al., 2023), there are limited bibliographic references to modelling approaches to simulate the effect of the sea level - sewer network interaction at outfall level. The main reasons for this knowledge gap are various. Firstly, the limited general background on modelling of multi-hazard compound events, which has only gained attention in recent years (Zscheischler et al., 2018). Secondly, the intrinsic complexity behind the interaction between these two specific environments (the sea and

This project has received funding from the European Union's Horizon Europe research and innovation programme under grant agreement No. 101093806. The publication reflects only the authors' views and the European Union is not liable for any use that may be made of the information contained therein.

the sewer network) requires knowledge on both maritime engineering and urban drainage science (Lee et al., 2020).

Santiago-Collazo et al., (2019) developed a comprehensive review of modelling approaches to simulate compound event floodings in low-lying coastal areas. Despite not considering the role of sewer networks in any of the reviewed approaches, this document provides a good insight on the efforts devoted to this specific field of multi-hazard modelling. ***Table 1*** shown previously summarises the main modelisation approaches outlined by Santiago-Collazo et al., (2019) used to couple pluvial flooding and storm surge models.

The methodology proposed to assess the hazard posed by this specific multi-hazard event is based on a "one-way" coupling approach of a pluvial flooding and storm surge model.

It is articulated by defining abnormal boundary conditions in the outfalls of the urban drainage models, representing an increased water level in this point of the system during a storm surge. These conditions are determined with a hydrostatic extreme sea level model. Such approach allows to simulate key processes leading to floods during combined extreme rainfall and storm surge events.

1. Intrusion of seawater inside the pipes resulting in a partial or complete flooding of the downstream part of the sewer network reducing its drainage capacity.
2. Flooding of low-lying coastal areas due to the temporary rise of the sea level.

The flowchart (***Figure 24***) represents the data flow between the coupled single-hazard models.

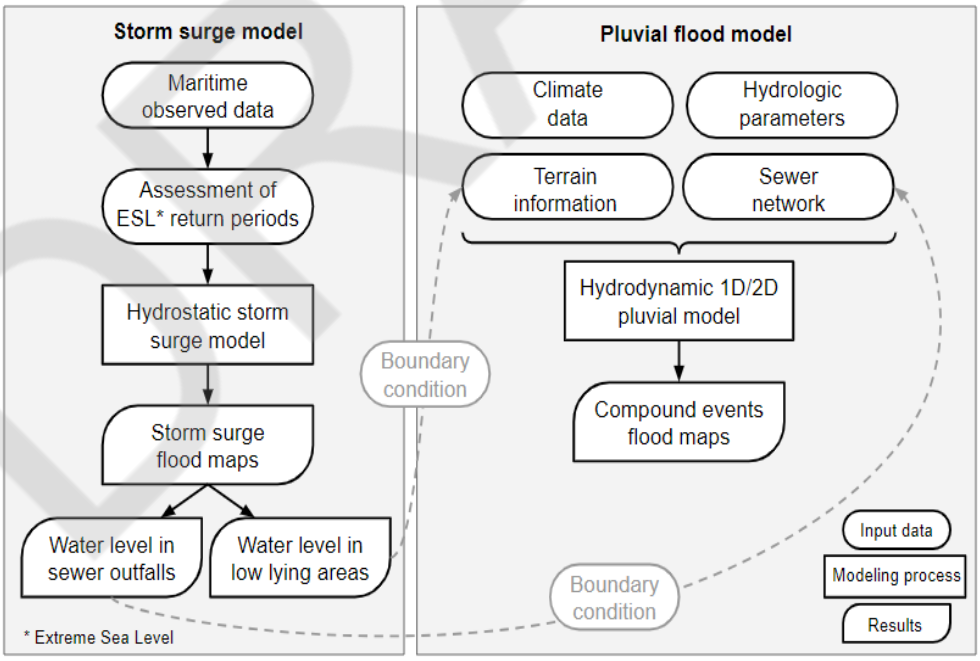

Figure 24. Flowchart of the one-way coupled approach to link pluvial flood and storm surge models.

This project has received funding from the European Union's Horizon Europe research and innovation programme under grant agreement No. 101093806. The publication reflects only the authors' views and the European Union is not liable for any use that may be made of the information contained therein.

The proposed approach allows a realistic modelling of the physical interaction between seawater and rain in the two key areas where they interact: the lower part of sewer networks whose outfalls have the sea as the water receiving body and low-lying coastal areas. However, it also requires especially accurate topographic surveys of the system outfalls and the overtopping height of the point where water is discharged to the sea as well as a high-resolution digital terrain model. Remarkably, information regarding the sewer network is often limited and/or inaccurate due to the usual data scarcity in the field of urban drainage infrastructure (Montalvo et al., 2024).

Similar approaches have been followed by other researchers like Lee et al. (2020), Jo et al. (2021), Qiang et al. (2021b), and Long and Gao (2023). ***Figure 25*** shows a conceptual model of an outfall connected to the sea under different rainfall and storm surge conditions to illustrate the mentioned interactions between wastewater and seawater sewer outfalls. ***Figure 26*** shows another conceptual model reflecting the second key boundary condition to consider in this multi-hazard modelling approach. The three scenarios represented illustrate how low coastal low-lying areas can be affected by extreme rainfall events, storm surges and their combined occurrence.

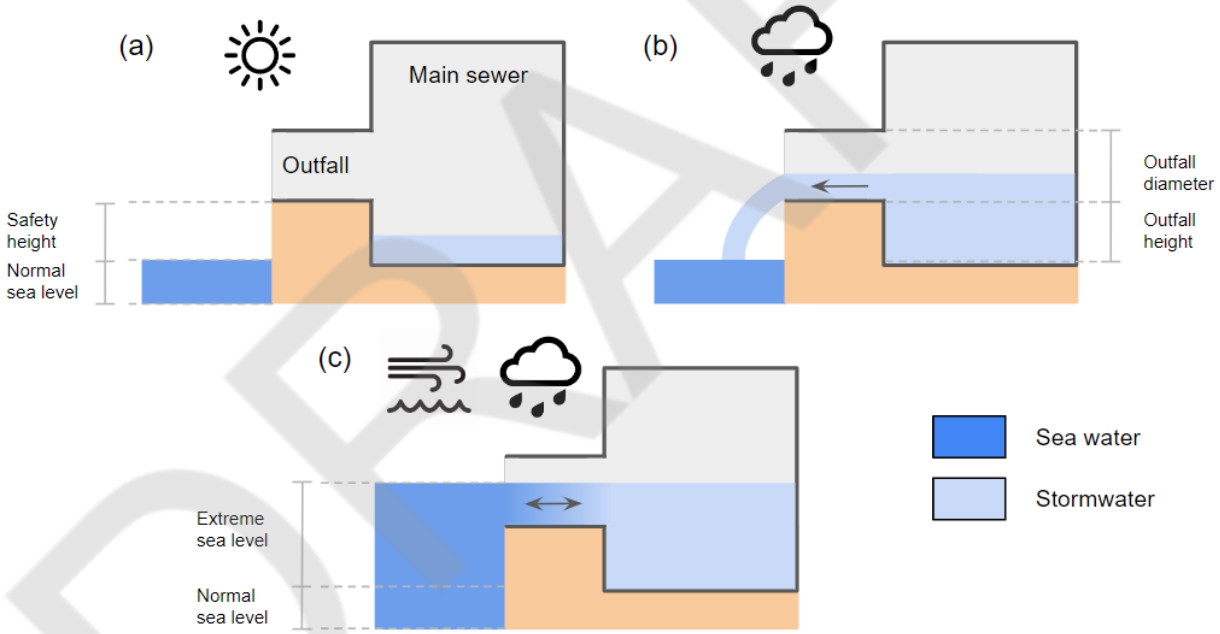

Figure 25. Scheme of an outfall connected to the sea under different conditions: (a) normal operation in dry weather conditions, (b) CSO due to an extreme rain event; (c) coincident storm surge and CSO.

This project has received funding from the European Union's Horizon Europe research and innovation programme under grant agreement No. 101093806. The publication reflects only the authors' views and the European Union is not liable for any use that may be made of the information contained therein.

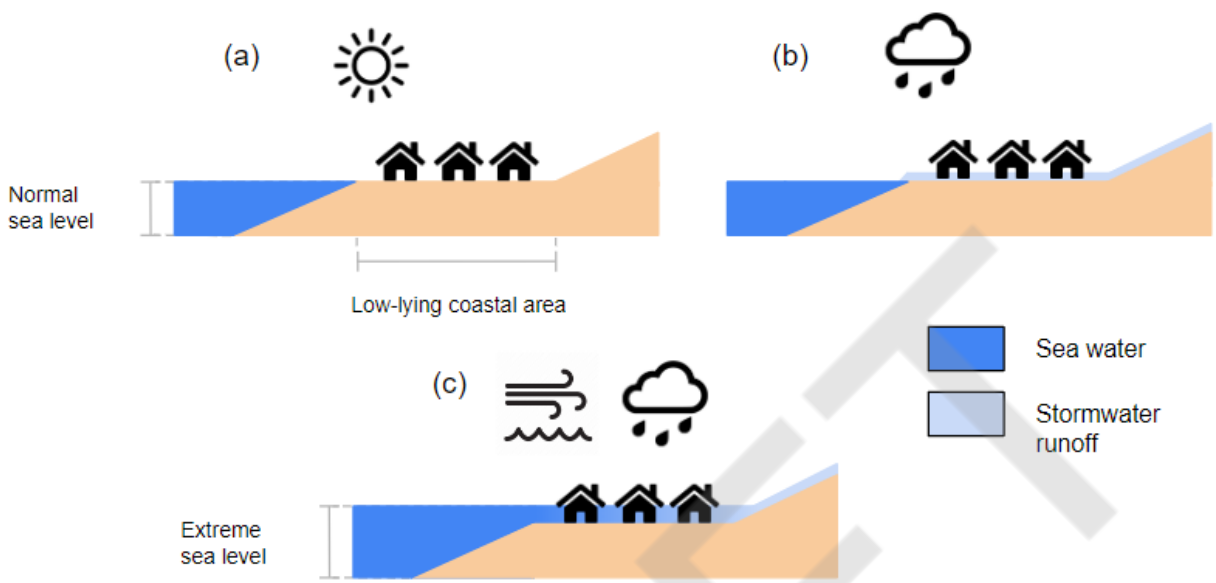

Figure 26. Scheme of a low-lying coastal area under different conditions: (a) dry weather conditions, (b) extreme rainfall conditions; (c) coincident coincidence storm surge and extreme rainfall conditions.

The following bullet points present the main steps to follow to set up the one-way coupled multi-hazard model shown in ***Figure 24*** to simulate compound events combining pluvial flooding and storm surge. These should not be understood as a thorough step-by-step guide, but as a guide of the main processes to be followed.

1. Set up a hydrostatic storm surge model to assess the water height above the normal sea level reached during transitory extreme sea level events (Crisi-Adapt II 2020; ICARIA 2023b).
2. Extract extreme sea level values for different events of reference (corresponding to different percentiles of rainfall intensity associated to specific return periods)
3. Set up an hydrodynamic 1D/2D urban drainage model of the area of study (ICARIA 2023b).
4. Define the model boundary conditions based on the results of the previous step. These boundary conditions have to be defined at two levels (see ***Figure 24*** to ***Figure 26***).
    a. Boundary condition for the 2D domain of the pluvial flooding level to represent the flooding of coastal areas due to the increased sea level.
    b. Boundary conditions in the sewer system outfalls to represent the backwater effect caused by the intrusion of seawater in the drainage network.
5. Simulate an extreme rainfall event with the 1D/2D hydrodynamic model considering the mentioned boundary conditions.

This project has received funding from the European Union's Horizon Europe research and innovation programme under grant agreement No. 101093806. The publication reflects only the authors' views and the European Union is not liable for any use that may be made of the information contained therein.

The results of the model correspond to a flooding map (showing water depth and velocity) resulting from the combined effect of the extreme rainfall and sea level.

The suggested approach presents a number of simplifications and data needs that generate uncertainty in the final results. ***Table 8*** summarises them and suggests possible uncertainty reduction measures.

Table 8. Main sources of uncertainty in the one-way coupled pluvial flooding and storm surge multi-hazard model and possible improvements.

Source of uncertainty	*Uncertainty reduction measure*
The data of outfalls structure and actual height above mean sea level is often inaccurate	Carry fieldwork to accurately characterise the dimensions and height above mean sea level
A simplistic model to assess the hazard conditions of storm surges in coastal areas is used	Consider using a hydrodynamic storm surge model capable to simulate wave dynamics
The boundary conditions introduced to represent the ESL in the outfalls are stationary values, which do not account the dynamic nature of storm surges	Define time-varying boundary conditions to represent the short-term fluctuations in the sea level at the sewer outfalls

5.1.2 Joint Probability Assessment

For the assessment of pluvial flooding and storm surge, compound coincident scenarios have been considered the influence of storm surge on the boundary conditions of the pluvial flood model. To assess the joint probability of these events, analysis will be undertaken on the correlation of days with extreme rainfall and that correspond to days where there are significant storm surge events. With these events being potentially correlated, the historical data relating to storm surge and extreme rainfall days will be analysed. Based on this assessment, probability of compound coincident events will be defined either relating to Copula based derived return periods (where there is correlation).

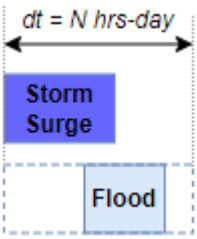

Figure 27. Temporal depiction of modelling of pluvial flood events during a storm surge.

This project has received funding from the European Union's Horizon Europe research and innovation programme under grant agreement No. 101093806. The publication reflects only the authors' views and the European Union is not liable for any use that may be made of the information contained therein.

However, if observations are absent, a dependence parameter will have to be assumed (independent, modestly correlated, well correlated, strongly correlated, super correlated) in order to use the JOIN-SEA analysis method for estimating the joint-probability and testing the sensitivity of the correlations between the variables (Hawkes and Svensson, 2005).

Table 9 and ***Table 10*** show the median and 90th percentile estimations of 1.1, 5, 10, 50, 100 and 500 year return periods storm surge height, derived from the SSP 126 and SSP 585, for 2015-2040, 2041-2070 and 2071-2010 time horizon. The SSP 126 median projection has a greater storm surge height during 2015-2040 than other median projections, while for the 90th percentile estimations, the SSP 126 projection show an extreme storm surge during 2041-2070 time horizon.

Table 9. Median estimation of 1.1, 5, 10, 50, 100 and 500 year return period daily rainfall for Barcelona region under SSP 126 and SSP 585 scenarios.

Return Period (Years)	SSP 126 Storm Surge (m)			SSP 585 Storm Surge (m)		
	2015-2040	2041-2070	2071-2100	2015-2040	2041-2070	2071-2100
1.1	2.99	3.19	3.18	3.25	3.17	2.92
5	4.09	4.03	3.99	4.02	3.94	3.93
10	4.28	4.20	4.15	4.17	4.11	4.12
50	4.67	4.55	4.47	4.45	4.46	4.52
100	4.82	4.69	4.59	4.57	4.61	4.68
500	5.14	5.00	4.87	4.82	4.94	5.03

Table 10. 90th percentile estimation of 1.1, 5, 10, 50, 100 and 500 year return period daily rainfall for Barcelona region under SSP 126 and SSP 585 scenarios.

Return Period (Years)	SSP 126 Storm Surge (m)			SSP 585 Storm Surge (m)		
	2015-2040	2041-2070	2071-2100	2015-2040	2041-2070	2071-2100
1.1	3.48	3.73	3.64	3.75	3.59	3.48
5	5.20	5.35	5.10	5.10	5.10	4.98
10	5.55	5.81	5.41	5.37	5.45	5.32
50	6.26	6.94	6.08	5.91	6.21	6.04
100	6.55	7.48	6.35	6.13	6.53	6.34
500	7.18	8.90	6.97	6.61	7.28	7.03

This project has received funding from the European Union's Horizon Europe research and innovation programme under grant agreement No. 101093806. The publication reflects only the authors' views and the European Union is not liable for any use that may be made of the information contained therein.

Figure 28 shows the estimated 1.1, 2, 5, 10, 30, 50, and 100 year return periods daily rainfall using 4 SSPs (126, 245, 370, and 585), each includes 10 climate models (MPI-ESM1-2-HR, BCC-CSM2-MR, CanESM5, CMCC-ESM2, EC-EARTH3, NorESM2-MM, ACCESS-CM2, CNRM-ESM2-1, MRI-ESM2-0, and UKESM1-0-LL), for Barcelona region. ***Table 11*** and ***Table 12*** list the median and 90th percentile estimations of daily rainfall with 1.1, 2, 5, 10, 30, 50, and, 100 year return period, derived from the 10 downscaled climate models under 4 SSPs. The results indicate that, comparing to historical period from 1950-2014, the average and extreme daily rainfall events are likely to decline in the future. But the daily rainfall for more frequent events, up to 30 year return period, may see greater amount of precipitation during 2015-2040 time horizon.

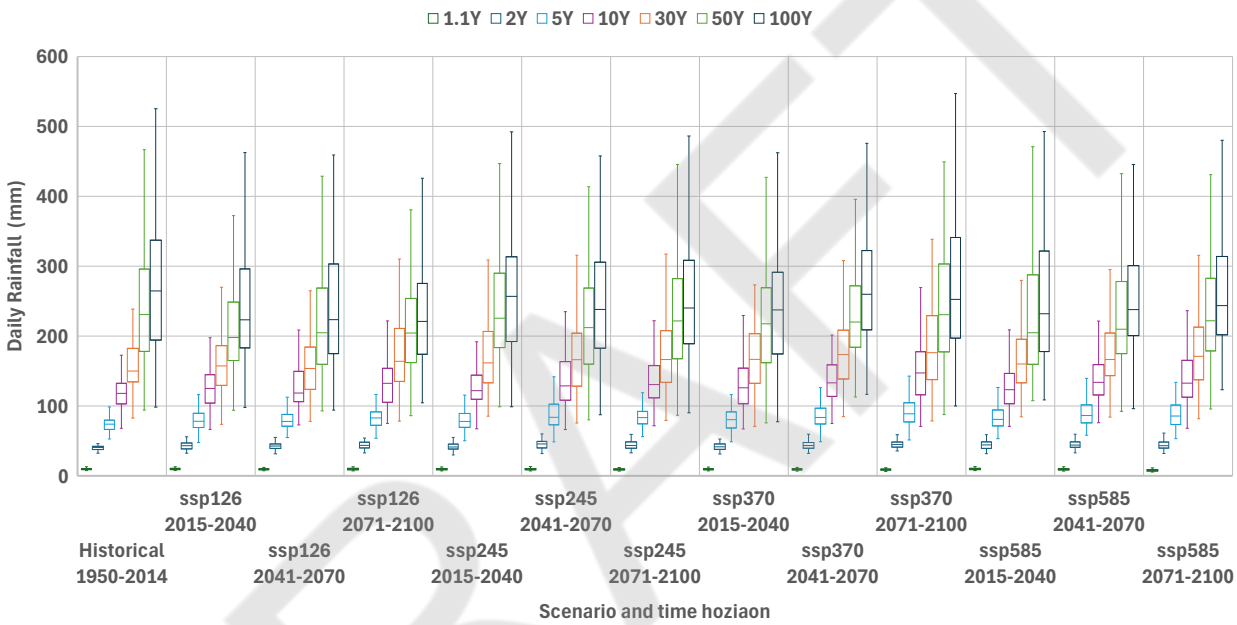

Figure 28. Daily rainfall distribution for 1.1, 2, 5, 10, 30, 50, and 100 year return periods using 4 SSPs (126, 245, 370, and 585), each includes 10 climate models (MPI-ESM1-2-HR, BCC-CSM2-MR, CanESM5, CMCC-ESM2, EC-EARTH3, NorESM2-MM, ACCESS-CM2, CNRM-ESM2-1, MRI-ESM2-0, and UKESM1-0-LL), for Barcelona region.

This project has received funding from the European Union's Horizon Europe research and innovation programme under grant agreement No. 101093806. The publication reflects only the authors' views and the European Union is not liable for any use that may be made of the information contained therein.

Table 11. Median estimation of 1.1, 2, 5, 10, 30, 50, and 100 year return period daily rainfall for Barcelona region derived from 4 SSPs (126, 245, 370, and 585), each includes 10 climate models (MPI-ESM1-2-HR, BCC-CSM2-MR, CanESM5, CMCC-ESM2, EC-EARTH3, NorESM2-MM, ACCESS-CM2, CNRM-ESM2-1, MRI-ESM2-0, and UKESM1-0-LL)

Return Period (Years)	Daily Rainfall (mm)			
	1950-2014	2015-2040	2041-2070	2071-2100
1.1	39.7	42.6	41.2	40.9
2	72.4	78.9	76.6	80.1
5	116.1	121.9	116.3	122.0
10	155.6	162.0	144.6	149.0
30	241.0	211.5	205.9	190.6
50	280.3	231.6	232.3	212.9
100	355.5	346.3	236.5	212.9

Table 12. 90th percentile estimation of .1, 2, 5, 10, 30, 50, and 100 year return period daily rainfall for Barcelona region derived from 4 SSPs (126, 245, 370, and 585), each includes 10 climate models (MPI-ESM1-2-HR, BCC-CSM2-MR, CanESM5, CMCC-ESM2, EC-EARTH3, NorESM2-MM, ACCESS-CM2, CNRM-ESM2-1, MRI-ESM2-0, and UKESM1-0-LL)

Return Period (Years)	Daily Rainfall (mm)			
	1950-2014	2015-2040	2041-2070	2071-2100
1.1	41.8	49.2	42.3	41.3
2	78.7	94.9	79.0	81.9
5	135.1	167.2	123.7	124.6
10	189.9	241.4	150.4	149.3
30	313.0	320.3	205.1	190.6
50	355.5	346.3	236.5	212.9
100	397.1	366.1	248.7	230.4

This project has received funding from the European Union's Horizon Europe research and innovation programme under grant agreement No. 101093806. The publication reflects only the authors' views and the European Union is not liable for any use that may be made of the information contained therein.

Figure 29 to ***Figure 34*** shows the Q50 and Q90 annual joint probability curves of storm surge height and daily rainfall for the Barcelona case for various periods under SSP 126 and SSP 585 scenarios. The availability of observation data did not allow the use of the Copula approach in the assessment such that the JOIN-SEA method was applied. This will require the assumption of the correlations between the storm surge height and daily rainfall, which is described as a correlation coefficient ρ (Hawkes and Svensson, 2005). If $\rho > 0.7$, the two variables are considered as highly dependent. One the other hand, if $\rho \leq 0.11$, the variables can be considered as independent. For $0.38 \leq \rho \leq 0.53$, the variables are well correlated. In the study, three ρ values were tested to evaluate how the correlation between storm surge height and daily rainfall could affect the results.

Figure 29 and ***Figure 30*** are the Q50 and Q90, respectively, with $\rho = 0.1$ between the storm surge height and rainfall. In this case, the two variables are considered as independent such that the joint probability for both variables having extreme high values is low. An Q50 event with 1000-year return period may have a storm surge height 2.92 - 3.18m and daily rainfall 116 – 125 mm. ***Figure 31*** and ***Figure 32*** are the ones with $\rho = 0.4$, the variables are well correlated such that a Q50 1000-year return period event may have storm surge 3.93-4.09 m and daily rainfall 160-166 mm. ***Figure 33*** and ***Figure 34*** are the ones with $\rho = 0.7$, the variables are highly correlated such that a Q50 500-year return period event will have storm surge 3.93-4.09 m and daily rainfall 222-225 mm.

This project has received funding from the European Union's Horizon Europe research and innovation programme under grant agreement No. 101093806. The publication reflects only the authors' views and the European Union is not liable for any use that may be made of the information contained therein.

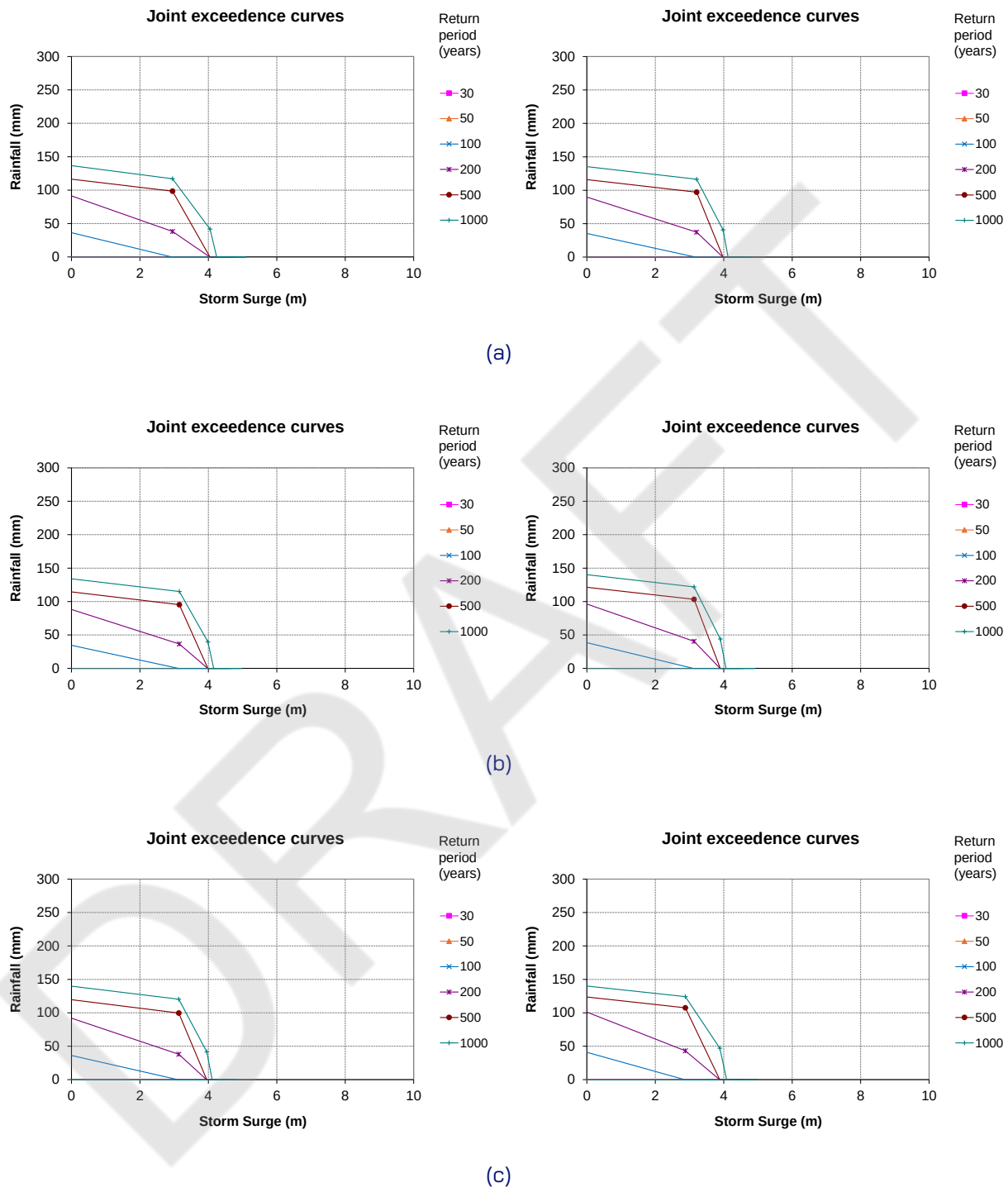

Figure 29. Q50 percentile storm surge and daily rainfall joint annual probability contours of (dependence measure $\rho = 0.1$) Barcelona under SSP 126 (left) and SSP 585 (right) for (a) 2015-2040, (b) 2041-2070, and (c) 2071-2100 period

This project has received funding from the European Union's Horizon Europe research and innovation programme under grant agreement No. 101093806. The publication reflects only the authors' views and the European Union is not liable for any use that may be made of the information contained therein.

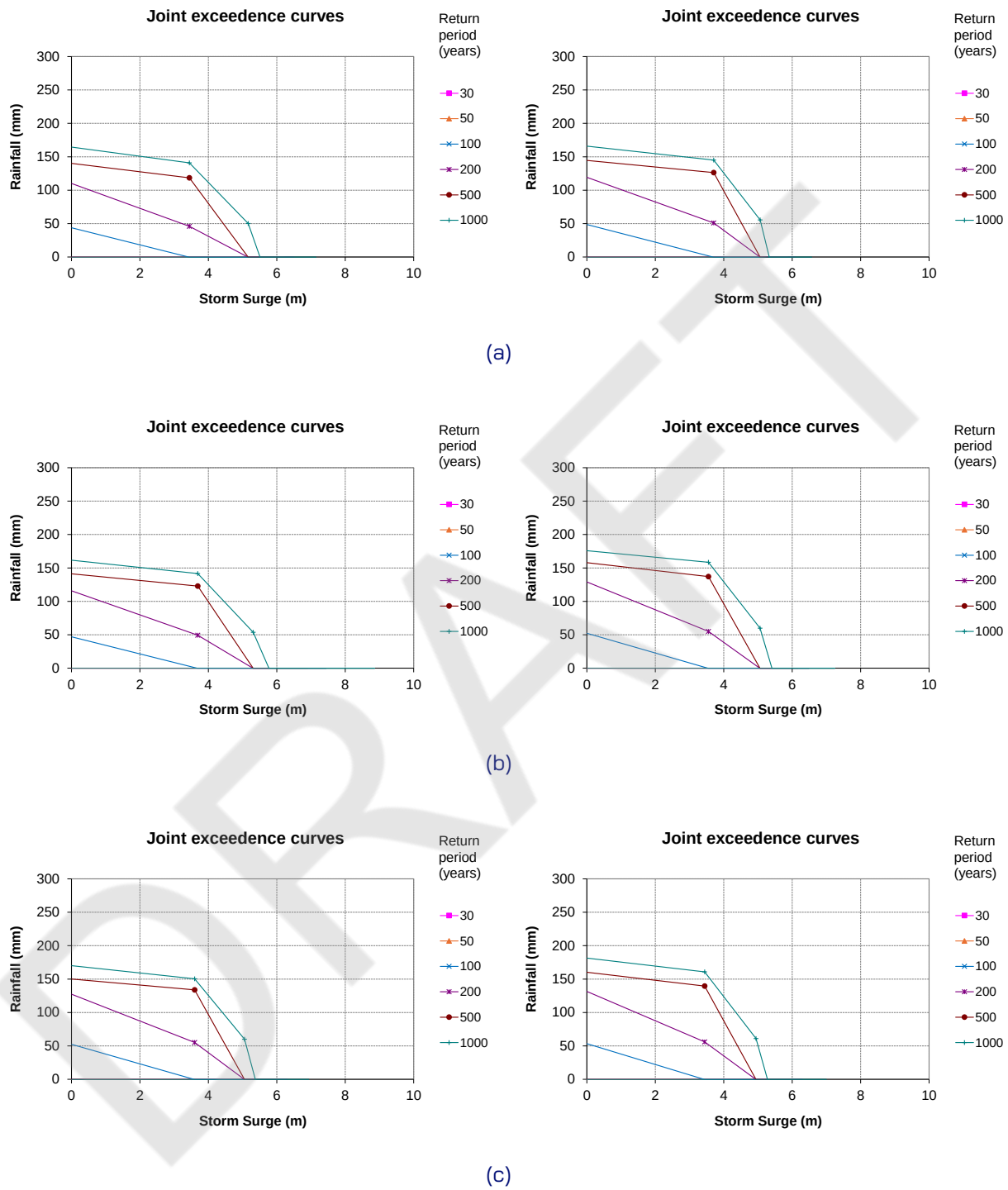

Figure 30. Q90 percentile storm surge and daily rainfall joint annual probability contours (dependence measure $\rho = 0.1$) of Barcelona under SSP 126 (left) and SSP 585 (right) for (a) 2015-2040, (b) 2041-2070, and (c) 2071-2100 period

This project has received funding from the European Union's Horizon Europe research and innovation programme under grant agreement No. 101093806. The publication reflects only the authors' views and the European Union is not liable for any use that may be made of the information contained therein.

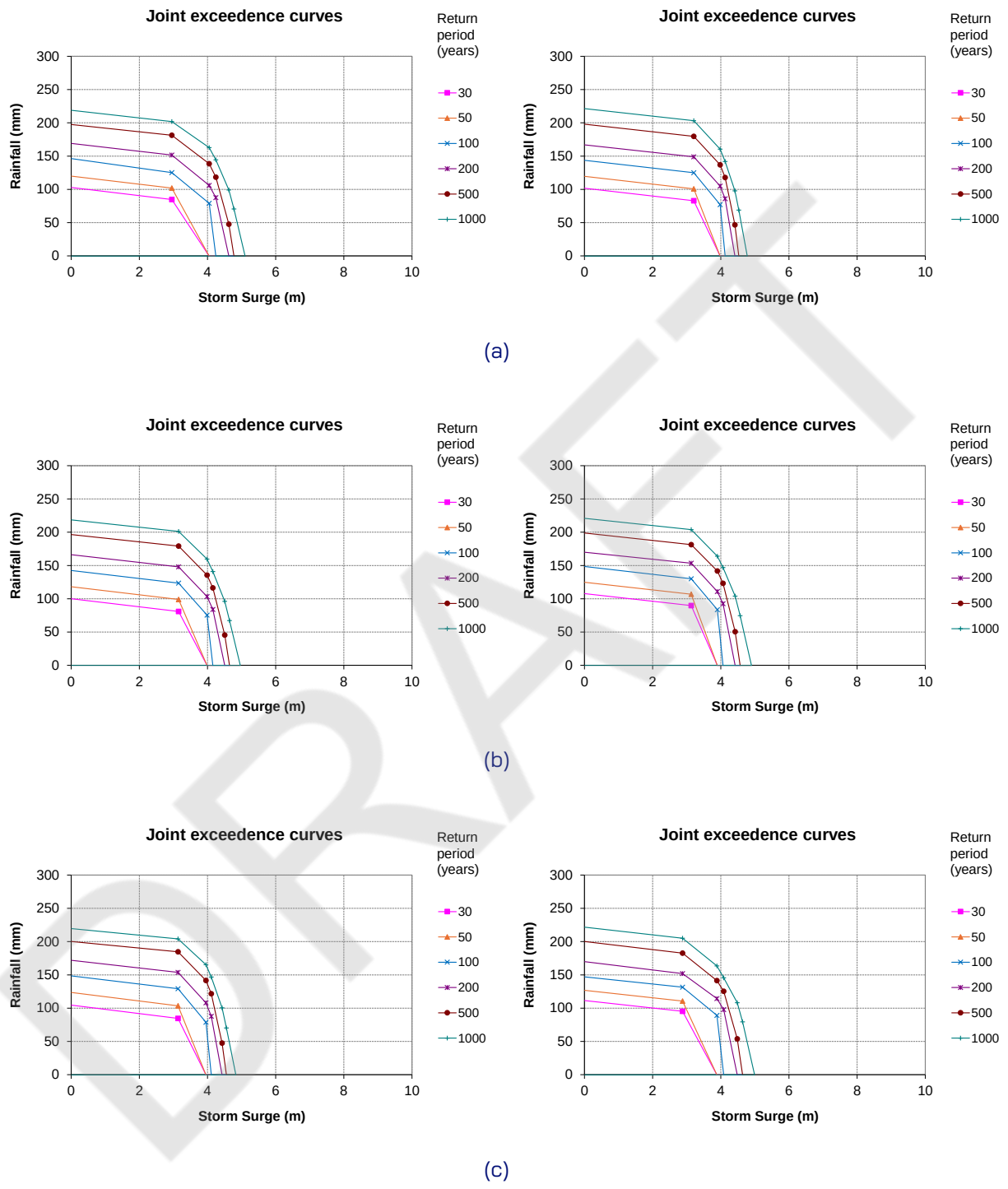

Figure 31. Q50 percentile storm surge and daily rainfall joint annual probability contours (dependence measure $\rho = 0.4$) of Barcelona under SSP 126 (left) and SSP 585 (right) for (a) 2015-2040, (b) 2041-2070, and (c) 2071-2100 period

This project has received funding from the European Union's Horizon Europe research and innovation programme under grant agreement No. 101093806. The publication reflects only the authors' views and the European Union is not liable for any use that may be made of the information contained therein.

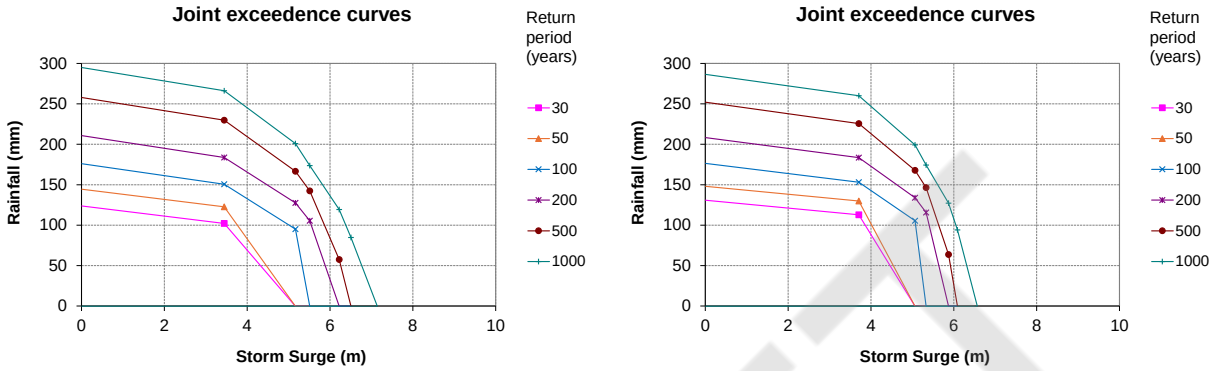

(a)

(b)

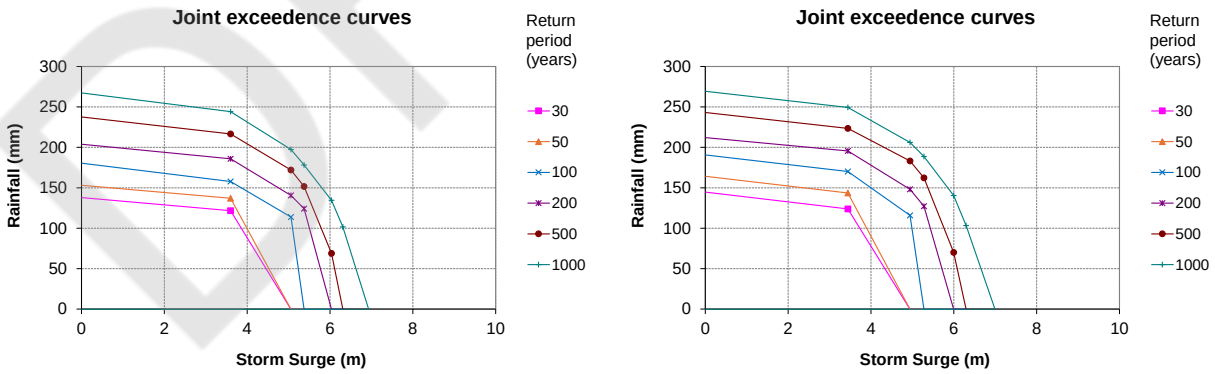

(c)

Figure 32. Q90 percentile storm surge and daily rainfall joint annual probability contours of (dependence measure $\rho = 0.4$) Barcelona under SSP 126 (left) and SSP 585 (right) for (a) 2015-2040, (b) 2041-2070, and (c) 2071-2100 period

This project has received funding from the European Union's Horizon Europe research and innovation programme under grant agreement No. 101093806. The publication reflects only the authors' views and the European Union is not liable for any use that may be made of the information contained therein.

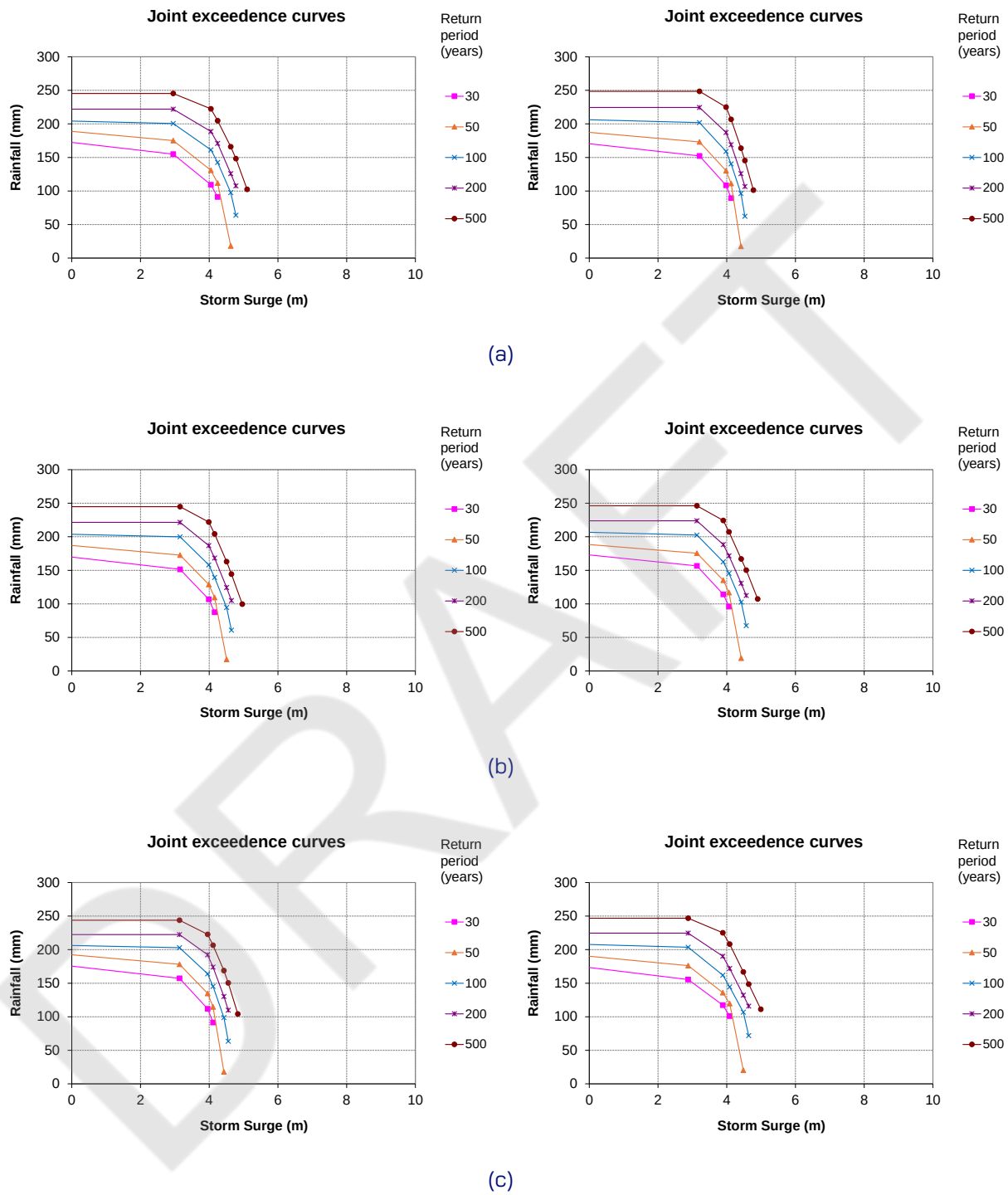

Figure 33. Q50 percentile storm surge and daily rainfall joint annual probability contours of (dependence measure $\rho = 0.7$) Barcelona under SSP 126 (left) and SSP 585 (right) for (a) 2015-2040, (b) 2041-2070, and (c) 2071-2100 period

This project has received funding from the European Union's Horizon Europe research and innovation programme under grant agreement No. 101093806. The publication reflects only the authors' views and the European Union is not liable for any use that may be made of the information contained therein.

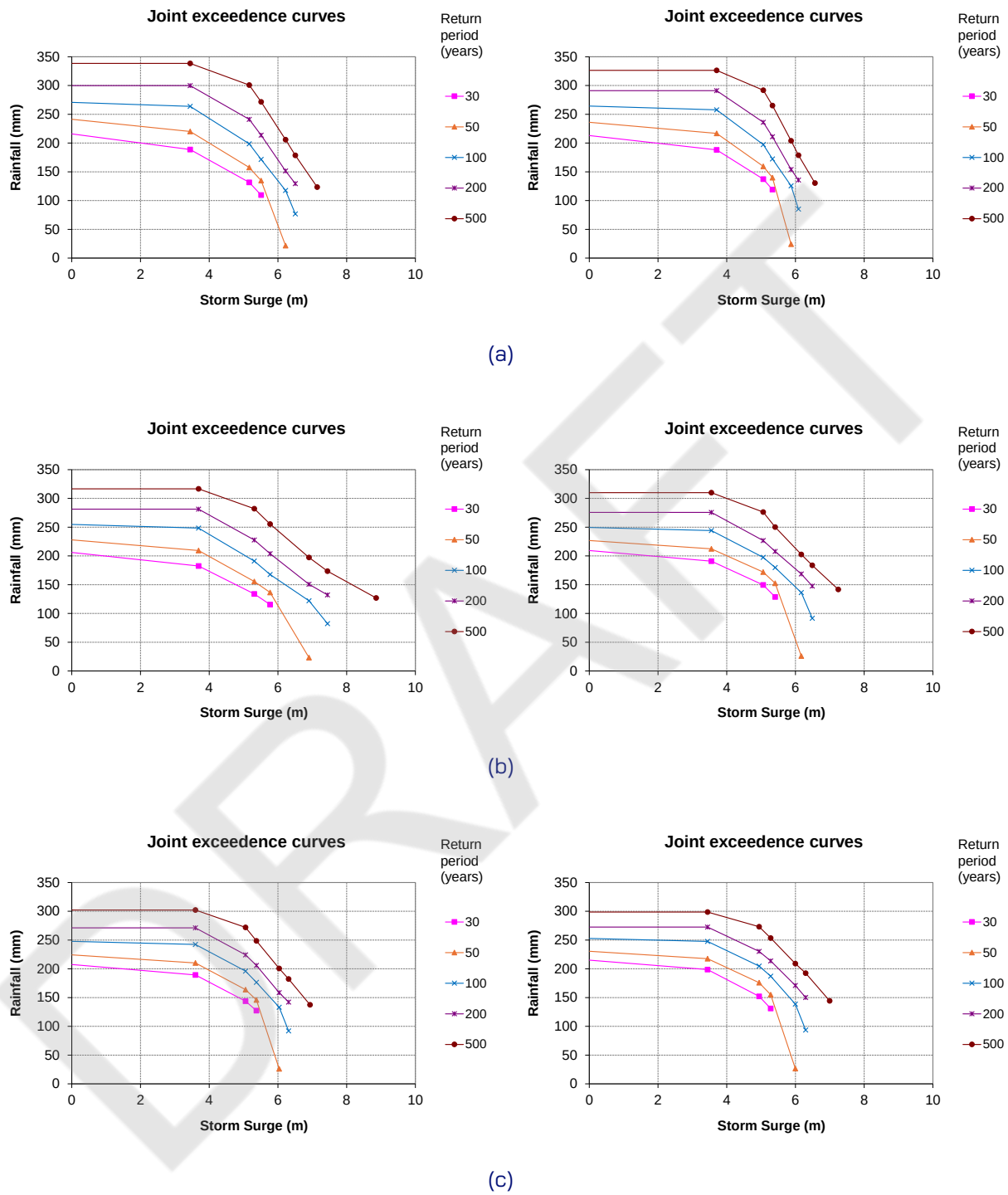

Figure 34. Q90 percentile storm surge and daily rainfall joint annual probability contours (dependence measure $\rho = 0.7$) of Barcelona under SSP 126 (left) and SSP 585 (right) for (a) 2015-2040, (b) 2041-2070, and (c) 2071-2100 period

This project has received funding from the European Union's Horizon Europe research and innovation programme under grant agreement No. 101093806. The publication reflects only the authors' views and the European Union is not liable for any use that may be made of the information contained therein.

5.2 Flooding and Extreme Wind

5.2.1 Compound Model setup

Compound events of flooding and extreme wind pose a risk to various types of natural and settlement areas. There are mainly two types of synoptic situations resulting in compound precipitation and storm events in Europe: (i) events that are caused by extratropical cyclones (Owen et al., 2021); (ii) summertime convective events (Pacey et al., 2021).

The recurrence time and magnitude of compound precipitation and wind extremes is predicted to increase under future conditions due to anthropogenic climate change (Ridder et al., 2022) and, especially, convective events will gain importance since warmer air can store more water, thereby causing increased precipitation intensities. At the level of physical interaction between hazards during coincident compound events, extreme rain events and windstorm do interact in the following ways:

1. Storms can increase the magnitude of flooding, trigger them through blocking the outflow of rivers and increase the probability of occurrence as storms alter the vulnerability of the surroundings towards extreme precipitation intensities.
2. In mountainous regions for instance, storms might lead to increased tree swamp, which causes increased inflow to the streams and decreased stability of the slopes. Both aspects affect flooding, the first one through blocked torrent barriers and therefore prevents the streams from flowing, the second increases the severity of extreme precipitation as destabilised slopes store less water, therefore increasing the runoff (Sebald et al., 2019).

It is important to note that flooding is considered as a hazard, not precipitation because extreme wind can trigger flooding, but can't trigger increased precipitation events.

Flooding cannot trigger storms, yet, a storm occurring after a flooding event might hit the region harder as it is already dealing with the consequences of the flooding.

To capture the effect of compound coincident or consecutive wind storms and flooding, a one-way coupling approach is taken (see ***Table 1***) whereby the influence of wind storms in the region on the conditions in the environment are modelled. Thus, the effect of the storm can be considered (depending on the type of stream, apparent flooding protection etc.) within the flooding model by:

- Adding a barrier within the stream downstream of a forest to represent the blocking due to trees
- Modelling the same precipitation event with a forested slope and a non-forested one to analyse the difference

These potential changes in conditions will thus be determined according to different maximum Wind Speeds with flooding events of different intensities, that are associated to their joint probabilities.

To simulate the flooding, the SFINCS model is used and the precipitation rates based on the dynamical model (SSP126, SSP585, 2 regional climate models, 2 - 5km spatial and hourly temporal resolution) are taken as input.

This project has received funding from the European Union's Horizon Europe research and innovation programme under grant agreement No. 101093806. The publication reflects only the authors' views and the European Union is not liable for any use that may be made of the information contained therein.

The wind gusts are taken from one of the regional climate models (CLM) which has wind gusts as output parameter, as well as from the WRF regional climate model but after post-processing steps as wind gusts are only partly available, but mean wind as well as wind at different pressure levels are. However, it is important to note that the maximum wind speed only indirectly affects the flooding model by defining the magnitude of broken trees.

5.2.2 Joint Probability Assessment

For defining the joint probability of Flooding and Extreme wind events within the Salzburg region, the probability of flood events occurring during (compound coincident) and after (compound consecutive) windstorm events are to be considered. To estimate the input parameters for respective return periods, both historical and future climate scenarios will be assessed.

For the compound consecutive hazard analysis, the probability of extreme rainfall events that follow extreme wind events are assessed over a various timeframe whereby assumptions will be required relating to recovery time of assets and the modelling environment based on expert knowledge and stakeholder discussions. The methodology has been described in Section 3.2.1 bivariate Copula Assessment.

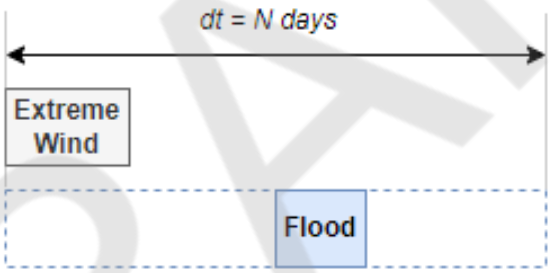

Figure 35. Temporal depiction of modelling of flood events during or following extreme wind.

This project has received funding from the European Union's Horizon Europe research and innovation programme under grant agreement No. 101093806. The publication reflects only the authors' views and the European Union is not liable for any use that may be made of the information contained therein.

Figure 36 shows the marginal distribution of projected daily rainfall and maximum wind speed by 2071-2099 under SSP 126 and ssp585 scenarios for Salzburg. Comparing to baseline scenario shown in ***Figure 9***, the magnitude of both hazards are likely to amplify in both SSP 126 and SSP 585, while the distribution pattern of rainfall will see higher ratio of extreme values under SSP 585.

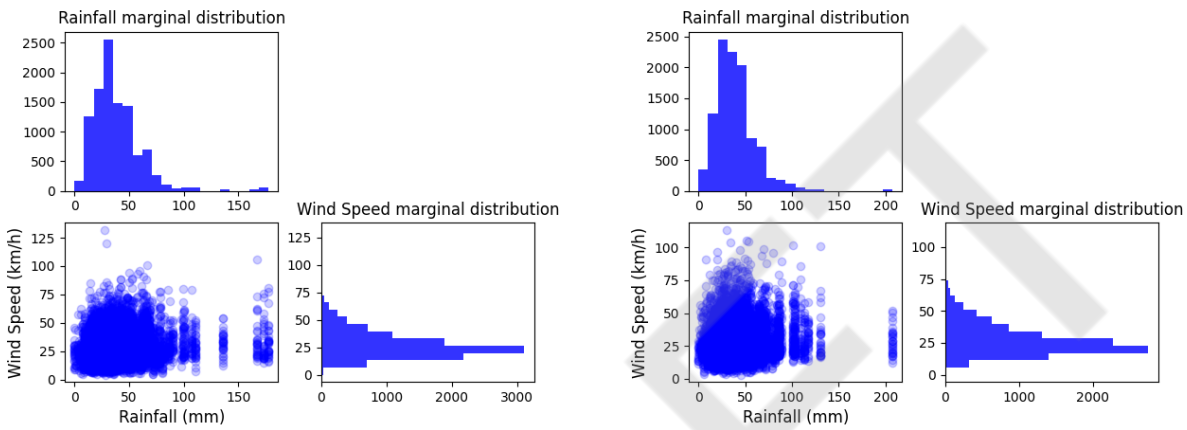

(a) (b)

Figure 36. Marginal distribution of daily rainfall and maximum wind speed for Salzburg under (a) SSP 126 and (b) SSP 585 scenarios (2071-2099).

Figure 37a shows that for SSP 126 scenario in period 2071-2099, coincident hazard events would have up to 55 mm daily rainfall and 68 km/h maximum wind speed has an annual joint probability 90%, while the daily rainfall may increase up to 160 mm and the maximum wind speed could reach 70 km/h under SSP 585 scenario with the same annual joint probability. Comparing to ***Figure 12***, for both historical and synthetic data, the daily rainfall is likely to be less than 15 mm and the maximum wind speed would be less than 12 km/h for coincident events.

Figure 37b and ***Figure 37***c show that if 7-day or 30-day time window is considered, the same 90% annual joint-probability could see more extreme daily rainfall and maximum wind speed. The result indicates substantial increases in the magnitude of both daily rainfall and maximum wind speed under future climate scenarios.

This project has received funding from the European Union's Horizon Europe research and innovation programme under grant agreement No. 101093806. The publication reflects only the authors' views and the European Union is not liable for any use that may be made of the information contained therein.

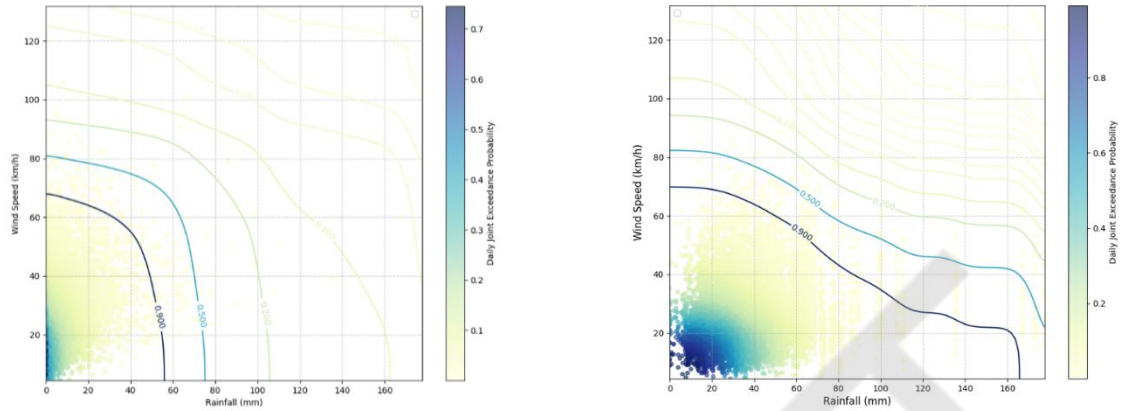

(a)

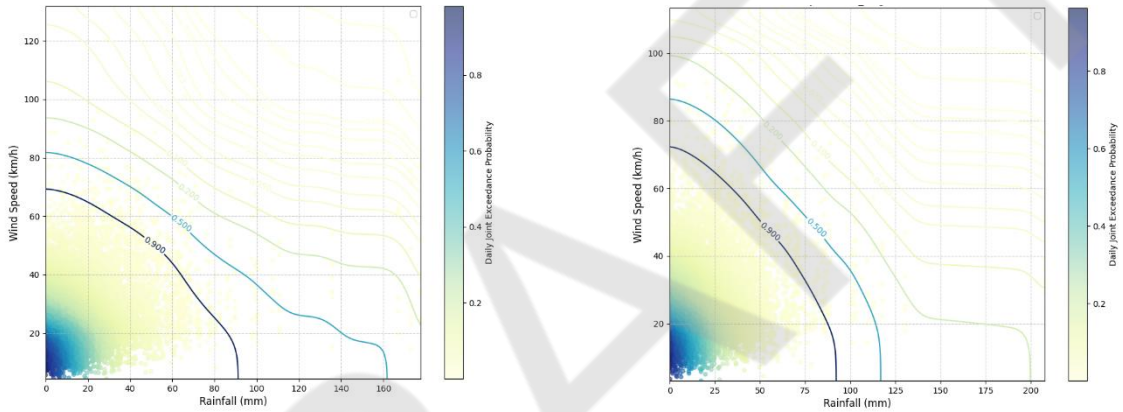

(b)

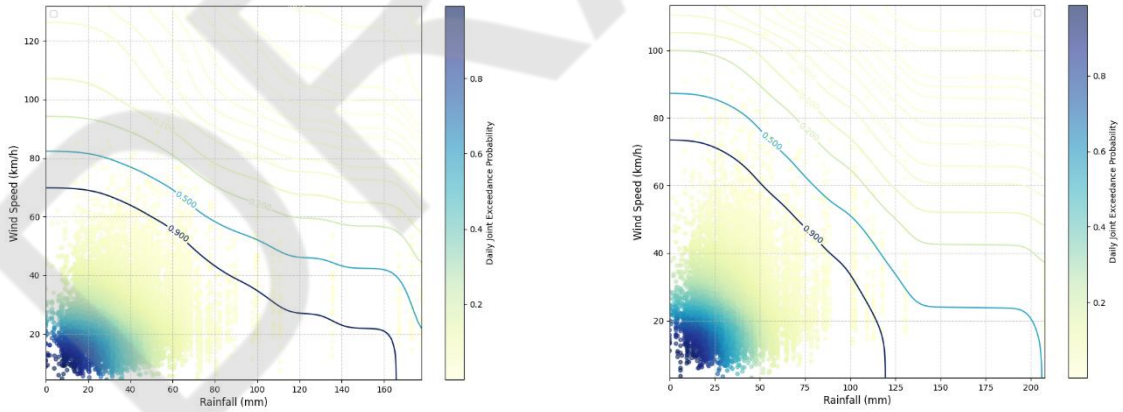

(c)

Figure 37. Daily joint probability of daily rainfall and maximum wind speed combinations (points), and the derived annual joint probability contours for the for Salzburg under SSP 126 (left) and SSP 585 scenarios (2071-2099) for (a) compound events, (b) consecutive events within a 7-day time window (c) consecutive events within a 30-day time window.

This project has received funding from the European Union's Horizon Europe research and innovation programme under grant agreement No. 101093806. The publication reflects only the authors' views and the European Union is not liable for any use that may be made of the information contained therein.

5.3 Extreme Wind and Forest Fire

5.3.1 Compound Model setup

The investigation of compound hazard events in terms of extreme wind and forest fire is analysed in this section, as a notable association exists between high fire risk and the presence of strong winds. It should be mentioned that the main hazard driver of this compound model is the fire hazard, described by the Fire Weather Index (FWI) and derived by the Canadian Forest Fire Weather Index (FWI) System. FWI is a meteorologically based index used worldwide to estimate fire danger. It consists of different components that account for the effects of fuel moisture and wind on fire behaviour and spread. The higher the FWI is, the more favourable the meteorological conditions to trigger a wildfire are. Their analytical presentation of the system equations and numerical codes describing the structure and components of the FWI system can be found in Wagner and Pickett (1984) (***Figure 38***). Calculation of the components is based on consecutive daily observations of temperature, relative humidity, maximum Wind Speed, and 24-hour precipitation.

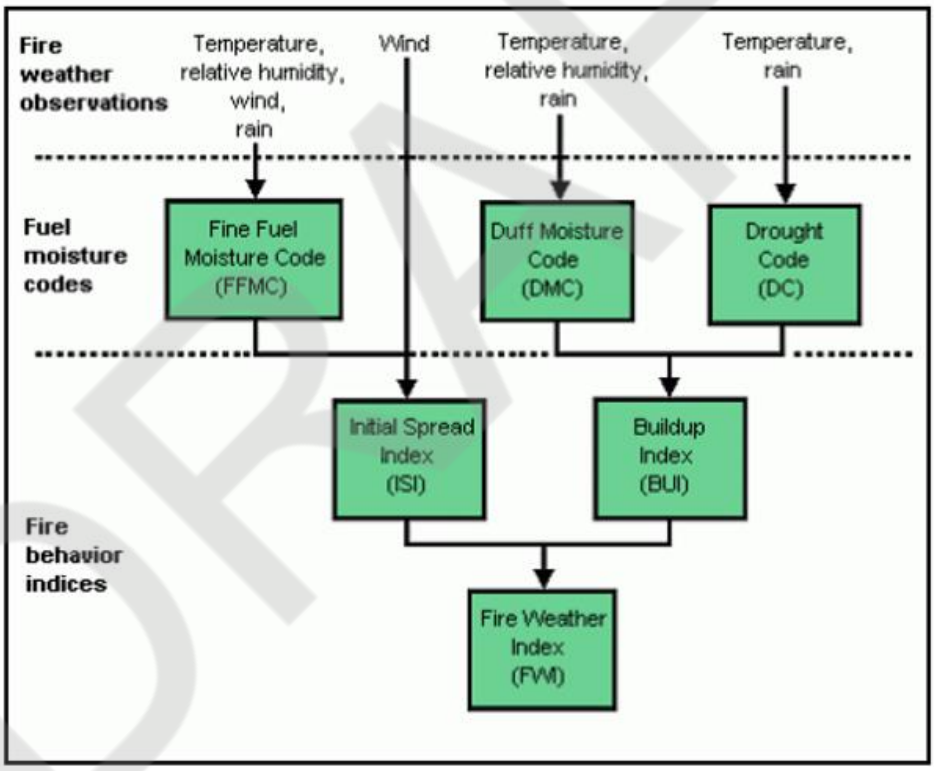

Figure 38. Structure of the FWI System (https://cwfis.cfs.nrcan.gc.ca/background/summary/fwi).

The first three components are fuel moisture codes, which are numeric ratings of the moisture content of the forest floor and other dead organic matter. Their values rise as the moisture content decreases. There is one fuel moisture code for each of the three layers of fuel: litter, represented by the moisture content of fine dead surface fuels (Fine Fuel Moisture Code, FFMC), loosely compacted organic material on the forest floor (Duff Moisture Code, DMC), and deep, compact organic soil layers (Drought Code, DC). The remaining three components are fire behaviour indices, which represent the rate of fire spread,

This project has received funding from the European Union's Horizon Europe research and innovation programme under grant agreement No. 101093806. The publication reflects only the authors' views and the European Union is not liable for any use that may be made of the information contained therein.

the fuel available for combustion and the frontal fire intensity. The FFMC is combined with maximum wind speed to estimate the potential spread rate of a fire (Initial Spread Index, ISI).

The Initial Spread Index (ISI) is a numeric rating of the expected rate of fire spread and one of the factors that hazard models have to take into consideration during extreme fire weather. The classification of the FWI and ISI components according to EFFIS is presented in ***Table 13***.

Table 13. Classification of values for the FWI and the ISI according to EFFIS (https://forest-fire.emergency.copernicus.eu/about-effis/technical-background/fire-danger-forecast).

Fire Danger Classes	*FWI*	*ISI*
Low	<11.2	< 5.0
Moderate	11.2 - 21.3	5.0 - 7.5
High	21.3 - 38.0	7.5 - 13.4
Very High	38.0 - 50	>=13.4
Extreme	50.0 - 70	
Very Extreme	>= 70	

Extreme Wind is a major controlling factor that determines rate and direction of spread, and shape of fire. The presence of strong winds plays a crucial role in determining wildfire behaviour by affecting their rapid spread, their intensity, turning the surface fires evolving into more severe crown fires with extreme fire behaviour and potentially making it more difficult to control fire (Zong et al., 2023, Richardson et al., 2022).

Within the ICARIA project, the compound hazard model will be set up for the selected area of study using the historical and future model datasets, which consist of 10 climate models each with 4 SSPs. The following description imposes the necessary steps for the definition of the coincidence of the compound events of forest fire and extreme winds:

- Calculation of daily FWI for fire season of each year for a given time period.
- Definition of the extreme fire danger FWI values using percentile values (e.g., 90th percentile of baseline) or selection from EFFIS extreme class threshold values for the selected location of interest for a given time period (e.g. for SAR region, FWI>70 is more representative for Greece as the extreme FWI is considered too low, and fire season spans from May to October).
- The daily coincidence of the selected FWI threshold with very high ISI (ISI >=13.4), along with extreme winds, exceeding the threshold 40km/h, in a daily time frame for each year for a given time period, represents the compound event of extreme winds and forest fire.
- Count of the annual number of days that fulfil the coincidence of the compound events.

This project has received funding from the European Union's Horizon Europe research and innovation programme under grant agreement No. 101093806. The publication reflects only the authors' views and the European Union is not liable for any use that may be made of the information contained therein.

- The results, as the median of ensemble models, are resumed to a table or a map that shows the number of days resulting from the combined effect of forest fires and extreme winds for the historical period and each climate change scenario for the selected case study.

The bivariate Copula Assessment described in Section 3.2.1 and the bivariate Copula with Linear Regression Assessment in Section 3.2.2 can be applied to derive the joint probability between the extreme wind and FWI.

5.3.2 Joint Probability Assessment

With wind being one of the components in deriving the FWI score, the analysis of influence of extreme wind and FWI scores will be based on compound coincident events, as shown in ***Figure 39***. The joint probability is derived through the analysis of such events whereby days within wildfire season (June - September) will be considered and the relationship between FWI scores and along with extreme maximum wind speed values of 40km/hr and above are considered.

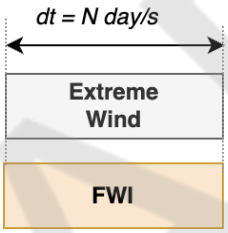

Figure 39. Temporal depiction of modelling influence of extreme wind on FWI scores.

Table 14 shows the annual joint probability of South Aegean Region with maximum wind speed exceeding 40 km/h and FWI exceeding baseline daily 90th percentile thresholds under baseline, SSP 126 and SSP 585 scenarios. However, the annual probability with maximum wind speed exceeding 40 km/h is 100% for KOS, NAXOS and SYROS such that the annual joint probabilities for baseline are 100% for baseline, SSP126 and SSP585 scenarios. For RODOS, the annual probability with a maximum wind speed exceeding 40 km/h is 95%, and the annual joint probabilities with a maximum wind speed exceeding 40 km/h and FWI exceeding baseline daily 90th percentile thresholds under baseline, SSP 126 and SSP 585 scenarios are greater than 76.9%. Thus, the selected thresholds were too low to represent extreme.

This project has received funding from the European Union's Horizon Europe research and innovation programme under grant agreement No. 101093806. The publication reflects only the authors' views and the European Union is not liable for any use that may be made of the information contained therein.

Table 14. The annual joint probability for maximum wind speed exceeding 40 km/h and FWI exceeding baseline daily 90th percentile thresholds for South Aegean Region for baseline, SSP 126 and SSP 585 scenarios.

Region	KOS	NAXOS	RODOS	SYROS
Wind speed threshold (km/h)	40	40	40	40
FWI baseline daily 90th percentile threshold	192.89	201.90	157.52	232.66
baseline annual joint probability (%)	100	100	91.4	100
SSP 126 2015-2040 annual joint probability (%)	100	100	76.9	100
SSP 126 2041-2070 annual joint probability (%)	100	100	94.6	100
SSP 126 2071-2099 annual joint probability (%)	100	100	97.1	100
SSP 585 2015-2040 annual joint probability (%)	100	100	76.9	100
SSP 585 2041-2070 annual joint probability (%)	100	100	87.1	100
SSP 585 2071-2099 annual joint probability (%)	100	100	98.7	100

DRAFT

This project has received funding from the European Union's Horizon Europe research and innovation programme under grant agreement No. 101093806. The publication reflects only the authors' views and the European Union is not liable for any use that may be made of the information contained therein.

Table 15 shows the annual joint probability of South Aegean Region with both maximum wind speed and FWI exceeding baseline daily 90th percentile thresholds under baseline, SSP 126 and SSP 585 scenarios. The annual probability corresponding to daily 90th percentile is 100%, and FWI is highly related to wind speed such that the threshold is unable to identify extreme windstorms and forest fire compound events. More restrictive thresholds were thus further tested.

Table 15. The annual joint probability for maximum wind speed exceeding baseline daily 90th percentile and FWI exceeding baseline daily 90th percentile thresholds for South Aegean Region for baseline, SSP 126 and SSP 585 scenarios.

Region	KOS	NAXOS	RODOS	SYROS
Wind speed baseline daily 90th percentile threshold (km/h)	43.36	44.41	35.26	49.88
FWI baseline daily 90th percentile threshold	192.89	201.90	157.52	224.12
baseline annual joint probability (%)	100	100	100	100
SSP 126 2015-2040 annual joint probability (%)	100	100	100	100
SSP 126 2041-2070 annual joint probability (%)	100	100	100	100
SSP 126 2071-2099 annual joint probability (%)	100	100	100	100
SSP 585 2015-2040 annual joint probability (%)	100	100	100	100
SSP 585 2041-2070 annual joint probability (%)	100	100	100	100
SSP 585 2071-2099 annual joint probability (%)	100	100	100	100

Table 16 and ***Table 17*** show the annual joint probability of South Aegean Region with maximum wind speed exceeding baseline daily 95th and 99th percentile, respectively, and FWI exceeding baseline daily 90th percentile thresholds under baseline, SSP 126 and SSP 585 scenarios. The daily 95th and 99th percentiles correspond to 99.99% and 84.26% annual probability, respectively. As mentioned above, wind speed and FWI are highly correlated such that the annual joint probabilities for the daily 95th percentile, as shown in ***Table 16***, are close to 100%. For the daily 99th percentile, as shown in ***Table 17***, the joint annual probabilities for all areas under all scenarios are in the range between 40% – 94%. To evaluate extreme events, more criteria were applied to analyse the annual joint probabilities.

This project has received funding from the European Union's Horizon Europe research and innovation programme under grant agreement No. 101093806. The publication reflects only the authors' views and the European Union is not liable for any use that may be made of the information contained therein.

Table 16. The annual joint probability for maximum wind speed exceeding baseline daily 95th percentile and FWI exceeding baseline daily 90th percentile thresholds for South Aegean Region for baseline, SSP 126 and SSP 585 scenarios. (casd09)

Region	KOS	NAXOS	RODOS	SYROS
Wind speed baseline daily 95th percentile threshold (km/h)	47.12	51.01	37.73	55.15
FWI baseline 90th percentile threshold	192.89	201.90	157.52	224.12
baseline annual joint probability (%)	99.9	99.5	100	99.8
SSP 126 2015-2040 annual joint probability (%)	99.7	96.0	99.9	96.2
SSP 126 2041-2070 annual joint probability (%)	99.0	96.7	99.9	99.0
SSP 126 2071-2099 annual joint probability (%)	98.7	100	100	99.9
SSP 585 2015-2040 annual joint probability (%)	100	99.6	99.8	99.4
SSP 585 2041-2070 annual joint probability (%)	97.8	98.8	99.8	98.4
SSP 585 2071-2099 annual joint probability (%)	99.8	99.9	100	99.8

DRAFT

This project has received funding from the European Union's Horizon Europe research and innovation programme under grant agreement No. 101093806. The publication reflects only the authors' views and the European Union is not liable for any use that may be made of the information contained therein.

Table 17. The annual joint probability for maximum wind speed exceeding baseline daily 99th percentile and FWI exceeding baseline daily 90th percentile thresholds for South Aegean Region for baseline, SSP 126 and SSP 585 scenarios. (case11)

Region	KOS	NAXOS	RODOS	SYROS
Wind speed baseline daily 99th percentile threshold (km/h)	51.3	61.04	40.70	62.23
FWI baseline daily 90th percentile threshold	192.89	201.90	157.52	224.12
baseline annual joint probability (%)	65.6	48.6	71.2	75.9
SSP 126 2015-2040 annual joint probability (%)	44.1	25.2	67.3	41.4
SSP 126 2041-2070 annual joint probability (%)	59.6	55.3	88.7	36.4
SSP 126 2071-2099 annual joint probability (%)	72.9	96.3	94.6	60.9
SSP 585 2015-2040 annual joint probability (%)	40.7	33.4	72.0	20.7
SSP 585 2041-2070 annual joint probability (%)	65.3	50.6	80.0	53.0
SSP 585 2071-2099 annual joint probability (%)	97.2	93.8	94.0	79.1

Table 18 shows the annual joint probability of South Aegean Region with maximum wind speed and FWI both exceeding baseline 20 % annual probability thresholds, respectively, under baseline, SSP 126 and SSP 585 scenarios. The 20% annual probability corresponding to daily 99.88th percentile thresholds. ***Table 18*** shows that the annual joint probabilities for SSP 126 and SSP 585 scenarios in South Aegean Region are likely to be greater than the baseline scenario for NAXOS and RODOS but KOS and SYROS have greater joint annual probability for the extreme events than SSP126 and 2015-2040 period for SSP585. ***Figure 40***b shows that the daily wind speed data in NAXOS and SYROS have higher ratio of lower values under SSP 126 scenarios than the ones under baseline (***Figure 40***a) and SSP 585 (***Figure 40***c) scenarios such that the joint probability for extreme events are lower.

This project has received funding from the European Union's Horizon Europe research and innovation programme under grant agreement No. 101093806. The publication reflects only the authors' views and the European Union is not liable for any use that may be made of the information contained therein.

Table 18. The annual joint probability for both maximum wind speed and FWI exceeding baseline exceeding baseline 20% annual possibility thresholds for South Aegean Region for baseline, SSP 126 and SSP 585 scenarios. (case03)

Region	KOS	NAXOS	RODOS	SYROS
Wind speed baseline 20% annual probability threshold (km/h)	58.02	76.31	48.24	76.78
FWI baseline 20% annual probability threshold	274.29	380.88	198.77	399.05
baseline annual joint probability (%)	19.9	0.0	0.0	26.7
SSP 126 2015-2040 annual joint probability (%)	10.9	0.0	10.9	5.6
SSP 126 2041-2070 annual joint probability (%)	14.0	0.0	9.5	0.0
SSP 126 2071-2099 annual joint probability (%)	18.8	14.5	18.7	9.9
SSP 585 2015-2040 annual joint probability (%)	11.0	6.2	17.5	0.0
SSP 585 2041-2070 annual joint probability (%)	39.5	0.0	23.4	9.6
SSP 585 2071-2099 annual joint probability (%)	22.9	30.2	9.9	22.9

DRAFT

This project has received funding from the European Union's Horizon Europe research and innovation programme under grant agreement No. 101093806. The publication reflects only the authors' views and the European Union is not liable for any use that may be made of the information contained therein.

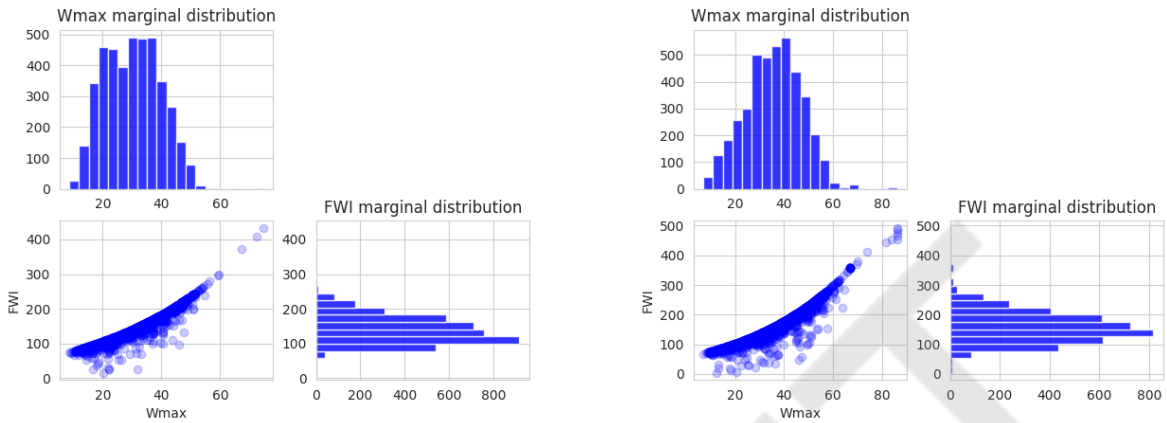

(a)

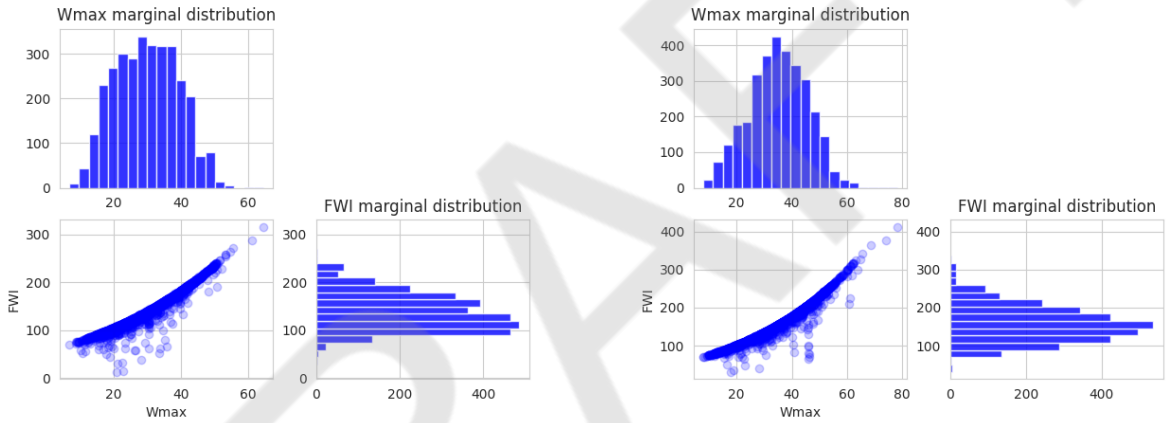

(b)

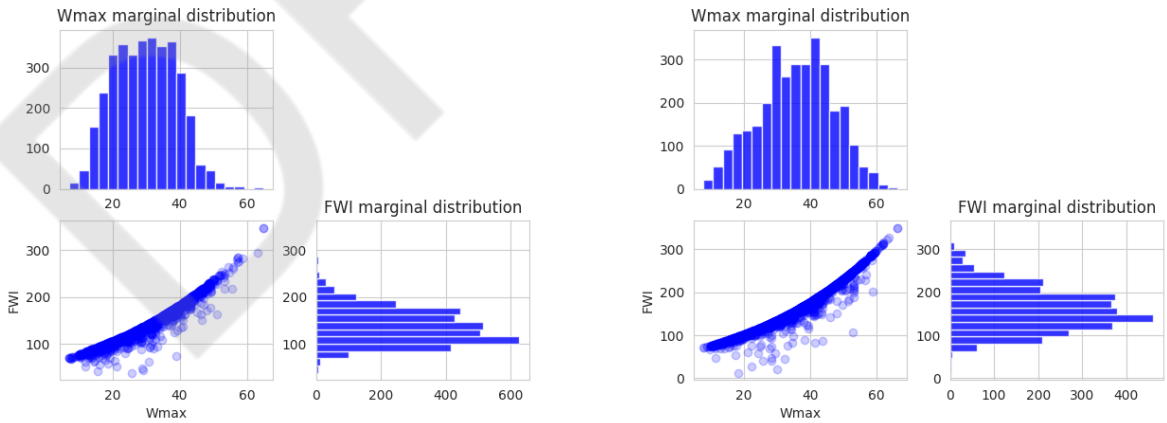

(c)

Figure 40. Marginal probability distribution of daily wind speed and FWI data for KOS (left) and SYROS (right) in South Aegean Region under (a) baseline, (b) 2015-2040 period in SSP 126 and (c) 2015-2040 period SSP 585 scenarios.

This project has received funding from the European Union's Horizon Europe research and innovation programme under grant agreement No. 101093806. The publication reflects only the authors' views and the European Union is not liable for any use that may be made of the information contained therein.

5.4 Drought and Heatwave

5.4.1 Compound Model setup

The effects of climate change are resulting in periods of higher extremes in relation to weather patterns. These extremes are reflected in the increasing occurrences of heatwaves and periods of drought. In the context of ICARIA, the combined effects of drought and heatwave will be assessed using a compound model set up whereby only events defined as heatwaves that occur within periods of drought (as highlighted in ***Figure 41***) are considered for the model climate parameters. Moreover, within the ICARIA project, the compound hazard model will be set up for the selected study area using the historical and future model datasets, consisting of 10 climate models each with 4 SSPs.

SPI6 calculation

The SPI is calculated by fitting a probability density function to a given frequency distribution of precipitation (Faye Cheikh et al. 2019) and then the probabilities are transformed into a normalised distribution with a mean equal to zero and a variance of one, developed by Mckee et al. (1993). The distribution function used for computing SPI was the 'Gamma' as the most widely used in literature and recommended. Moreover, the SPI-6 was selected for drought hazard modelling, as in semi-arid and arid regions (as the study area), drought index computed at shorter accumulation periods could give unreliable estimates (Karavitis et al 2014). Drought classification is provided in ***Table 19***. Moreover, drought conditions are indicated as SPI decreases below –1.0, while increasingly severe excess rainfall is indicated as SPI increases above 1.0.

Table 19. Drought classifications based on SPI.

Classification	*SPI*	*Drought classes*
1	SPI⩾2.00	extreme wet
2	2.00>SPI⩾1.50	very wet
3	1.50>SPI⩾1.00	moderate wet
4	1.00>SPI⩾-1.00	normal
5	-1.00⩾SPI>-1.50	moderate drought
6	-1.50⩾SPI>-2.00	severe drought
7	-2.00⩾SPI	extreme drought

This project has received funding from the European Union's Horizon Europe research and innovation programme under grant agreement No. 101093806. The publication reflects only the authors' views and the European Union is not liable for any use that may be made of the information contained therein.

The following description imposes the necessary steps for the definition of the coincidence of the compound events of drought and heatwave.

Definition of heatwave:

Within ICARIA and D1.2, a heatwave is defined as the period where the maximum daily temperature is equal to or exceeds the 95th percentile of summer (June, July, and August) temperatures for a duration of 3 or more consecutive days, for a given historical period.

Regarding the compound event drought and heatwave, the following approach will be used.

- Calculation of the monthly SPI6 as derived from the CMIP6 models for historical and future periods (for the selected SSPs) for the selected location.
    - Extraction of ***SPI6 of September*** values, for each year, which represent the drought conditions during the dry period in Greece.
    - Selection of drought years, based on the definition of drought conditions (-1.00⩾SPI) of ***Table 19***.
    - Statistical analysis and comparison of the number of heatwaves during these years in the historical and future period under the examined SSPs.

5.4.2 Joint Probability Assessment

The joint probability of these compound hazard events will consider the occurrence of heatwaves during periods of drought both in the historical context and range of future climate scenarios.

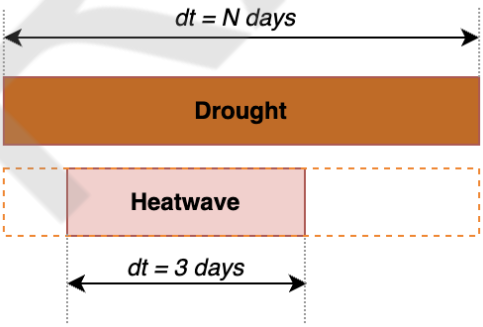

Figure 41. Temporal depiction of modelling heatwaves during periods of drought.

This project has received funding from the European Union's Horizon Europe research and innovation programme under grant agreement No. 101093806. The publication reflects only the authors' views and the European Union is not liable for any use that may be made of the information contained therein.

5.5 Drought and Forest Fire

5.5.1 Compound Model setup

Meteorological drought, which is generally defined as a period of unusual precipitation deficit, is not a necessary or sufficient condition for forest fire occurrence as fires also happen during conditions of normal seasonal aridity. However, when a drought occurs, both live and dead fuels can dry out and become more flammable and the probability of ignition increases along with rate of fire spread (Andrews et al., 2003; Scott & Burgan, 2005).

In the context of ICARIA, the combined effects of drought and forest fires will be assessed using a compound model set up. Moreover, within the ICARIA project, the compound hazard model will be set up for the selected area of study using the historical and future model datasets, which consist of 10 climate models each with 4 SSPs. For this compound model set up, it is primarily necessary the calculations of Standardised Precipitation Index (SPI) and Fire Weather Index (FWI) indices for the historical and future periods for selected locations, based on daily precipitation, maximum temperature, relative humidity and wind gust datasets.

The SPI is calculated by fitting a probability density function to a given frequency distribution of precipitation and then the probabilities are transformed into a normalised distribution with a mean equal to zero and a variance of one, developed by Mckee et al. (1993). The distribution function used for computing SPI was the 'Gamma' as the most widely used in literature and recommended.

Drought classifications for these compound scenarios are those that were previously defined in ***Table 19***.

As outlined earlier in the Extreme Wind and Forest Fire Section, the fire hazard is described by the Fire Weather Index (FWI), derived by the Canadian Forest Fire Weather Index (FWI) System with components defined in ***Figure 38*** with the corresponding Fire Danger Classes ranging from Low to Extreme (see ***Table 13***).

The Compound hazard model is represented by the following steps:

1. Calculation of the monthly SPI6 as derived from the CMIP6 models for historical and future periods (for the selected SSPs) for the selected location. The SPI6 was selected for drought hazard modelling, as in semi-arid and arid regions (as the study area), drought index computed at shorter accumulation periods could give unreliable estimates (Karavitis et al., 2014).
2. Calculation of the daily FWI for historical and future periods (for the selected SSPs) for the selected location.

After calculating both indices, it is important to define the common period for analysing the two indices in terms of compound hazards. This period is usually defined according to the fire season period representing each location. Eg May to October for SAR case study.

3. For the same period, the definition of the coincidence of the compound events includes the following final procedure:
    a. Extraction of ***SPI6 of October*** values, for each year, which represent the drought conditions of the entire fire season.
    b. ○ Selection of drought years, based on the definition of drought conditions (-1.00≥SPI) of ***Table 19***.

This project has received funding from the European Union's Horizon Europe research and innovation programme under grant agreement No. 101093806. The publication reflects only the authors' views and the European Union is not liable for any use that may be made of the information contained therein.

c. Statistical analysis and comparison of the extreme and mean values of the fire-related indices during these years in the historical and future period under SSPs:
    - Threshold of 90th percentile of FWI, ISI and FFMC
    - Number of very extreme fire days with FWI > 70.
    - Mean of FWI, FFMC and ISI

The output of the compound hazard model can be in the form of a table or map, depending on the type of datasets in point format or gridded.

5.5.2 Joint Probability Assessment

The joint probability of these compound hazard events will consider the probability distribution of fire danger weather during periods of drought.

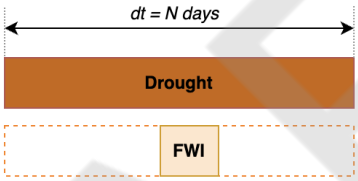

Figure 42. Temporal depiction of modelling FWI scores during periods of drought.

This project has received funding from the European Union's Horizon Europe research and innovation programme under grant agreement No. 101093806. The publication reflects only the authors' views and the European Union is not liable for any use that may be made of the information contained therein.

5.6 Heatwave and Forest Fire

5.6.1 Compound Model setup

Heatwaves and forest fires are hazards that are associated with each other, with their cooccurrence to have been increased the past decades, constituting in multi-hazard events. These events are mainly controlled by the duration and severity of the heatwaves. Prolonged high temperatures and dry conditions make vegetation more susceptible to the ignition of forest fires. The compound Heatwave – Forest fire hazard model needs as input the number and the duration of heatwaves along with the quantification of fire hazard during these heatwaves, represented by the Fire Weather Index (FWI).

Within ICARIA and D1.2, a heatwave is defined as the period, where the daily maximum temperature is equal to or exceeds the 95th percentile of summer (June, July, and August) temperatures for a duration of 3 or more consecutive days, for a given historical period.

The fire hazard is described by the Fire Weather Index (FWI), derived by the Canadian Forest Fire Weather Index (FWI) System with components defined in ***Figure 38*** with the corresponding Fire Danger Classes ranging from Low to Extreme (see ***Table 13***).

For the quantification of coincidence of these events the following methodology is applied.

Within ICARIA project, the compound hazard model will be set up for the selected area of study using the historical and future model datasets, which consist of 10 climate models each with 4 SSPs. The common period for the specific compound event is summer months (June – July – August) for the given historical or future period. For each year, a heatwave event and its duration are estimated, during the given period. Respectively, for every heatwave event that occurs, FWI values equal or greater than 70 or exceeding the extreme 90th percentile (Varela et al 2018) of the historical period, are extracted. This approach is applied also during the summer future period to examine the effect of combined events of heatwave and fire danger under climate change.

5.6.2 Joint Probability Assessment

Within the joint probability assessment of high FWI scenarios coinciding with heatwaves we need to consider the duration of the heatwave and the likelihood of "fire danger" during this period.

Within the scope of ICARIA the definition of a heatwave event as defined in D1.2 is an event where the temperature is equal to or exceeds 95th percentile of recorded summer (June, July, and August) temperatures during the period of 1981 - 2010 for a duration of 3 or more consecutive days.

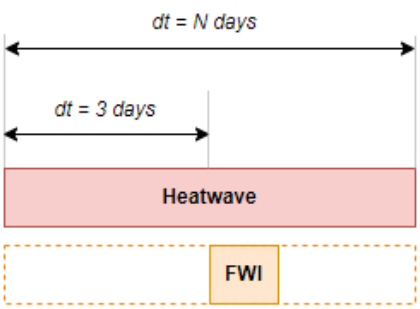

Figure 43. Defining compound Heatwave with Wildfire scenario.

This project has received funding from the European Union's Horizon Europe research and innovation programme under grant agreement No. 101093806. The publication reflects only the authors' views and the European Union is not liable for any use that may be made of the information contained therein.

For defining "fire danger" weather, common practice is to consider FWI scores equal or greater than 50, however within the region of Greece this value is considered too low, with an alternative being 90% annual probability within the modelled region. For consistency with the temperature metrics this 90% annual probability is derived over the same time period 1981 - 2010 however the months analysed for defining this threshold span May - October.

The bivariate Copula Assessment described in Section 3.2.1 can be applied to derive the joint probability between the extreme temperature and FWI.

Table 20 shows the annual joint probability in the four areas in South Aegean Region with 3 or more consecutive days having temperature higher than the baseline 95th percentile, followed by FWI exceeding the baseline 90th percentile. The substantial increase of annual probability under both SSP 126 and SSP 585 scenarios indicate that a greater risk of heatwave and forest fire compound events in the future. For RODOS, the 95th percentile thresholds seem to be too low to capture extreme compound events.

Table 20. The annual joint probability with 3 or more consecutive days that temperature exceeding 95th percentile of recorded summer temperatures during the period of 1981 – 2010, followed by FWI exceeding the 90th percentile of historical period during 1981-2010 baseline.

Region	*KOS*	*NAXOS*	*RODOS*	*SYROS*
Daily temperature baseline 95th percentile threshold	36.06	32.50	37.98	27.06
Daily FWI baseline 90th percentile threshold	192.89	201.90	157.52	224.12
baseline annual joint probability (%)	11.1	5.71	33.8	11.1
SSP 126 2015-2040 annual joint probability (%)	7.41	7.41	97.6	50.0
SSP 126 2041-2070 annual joint probability (%)	37.3	12.5	94.8	48.7
SSP 126 2071-2099 annual joint probability (%)	6.67	0	87.5	12.9
SSP 585 2015-2040 annual joint probability (%)	26.5	7.41	92.8	41.7
SSP 585 2041-2070 annual joint probability (%)	12.5	23.4	97.9	60.7
SSP 585 2071-2099 annual joint probability (%)	18.7	18.7	92.9	53.2

This project has received funding from the European Union's Horizon Europe research and innovation programme under grant agreement No. 101093806. The publication reflects only the authors' views and the European Union is not liable for any use that may be made of the information contained therein.

5.7 Heatwave, Drought and Forest Fire

5.7.1 Compound Model setup

The prolonged high temperature (heatwaves) and low precipitation periods (drought periods) increase the likelihood and magnitude of forest fire hazard.

Within ICARIA project, the compound hazard model will be set up for the selected area of study using the historical and future model datasets, which consist of 10 climate models each with 4 SSPs. The common period for the specific compound events is defined by the fire season that spans from May to October, for the given historical or future period.

This compound model involves analysing the effect of coincidence of heatwave, drought and forest fire, as defined by the Standardised Precipitation Index (SPI), heatwave definition and the Fire Weather Index (FWI). The first step requires the extraction of dry years based on the definition of drought conditions (-1.00⩾SPI). For each dry year, a heatwave event is estimated, where the maximum temperature is equal to or exceeds the 95th percentile of summer (June, July, and August) temperatures for a duration of 3 or more consecutive days, for a given historical period. Respectively, for every heatwave event that occurs, FWI values equal or greater than 70 or exceeding the extreme 90th percentile (Varela et al 2018) of the historical period, are extracted. This approach is applied also during the summer future period to examine the effect of combined events of heatwave, drought and fire under climate change.

5.7.2 Joint Probability Assessment

Like that of the previous combinations of drought, heatwave and FWI scores, this joint probability assessment will assess the likelihood and influence of drought, heatwaves, and FWI scores occurring within modelled regions for both historical and future scenarios.

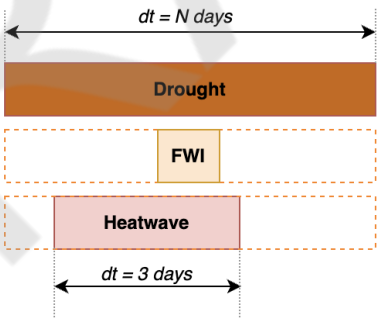

Figure 44. Defining compound Drought, Heatwave with Wildfire scenarios.

The multivariate Copula Assessment described in Section 3.2.3 could be applied to assess the joint probability between the extreme temperature, extreme wind and FWI. However, the limitation of the method may not be able to describe the relationships among three variables. Using the bivariate Copula Assessment in Section 3.2.1 or the bivariate Copula with Linear Regression Assessment in Section 3.2.2 for pairwise analysis may provide better results.

This project has received funding from the European Union's Horizon Europe research and innovation programme under grant agreement No. 101093806. The publication reflects only the authors' views and the European Union is not liable for any use that may be made of the information contained therein.

6. Conclusions

6.1 Summary

The work undertaken within Task 2.3: "Coupled hazard models: methodology and tools", this deliverable outlines the approaches used across the three case study regions for modelling multi-hazard scenarios" has outlined approaches for the coupling and modelling of seven compound hazard scenarios:

- Pluvial Flooding and Storm Surge
- Flooding and Extreme Wind
- Extreme Wind and Forest Fire
- Drought and Heatwave
- Drought and Forest Fire
- Heatwave and Forest Fire
- Drought, Heatwave, and Forest Fire

Across these compound hazard scenarios two generalised modelling approaches have been highlighted with:

- ***One-way coupling of models***: *Pluvial Flooding and Storm Surge,* Flooding and *Extreme Wind, Extreme Wind and Forest Fire, Heatwave and Forest Fire, and Drought, Heatwave and Forest Fire.*
- ***Statistical analysis of hazard drivers***: *Extreme Wind and Forest Fire*, *Drought and Heatwave, Drought and Forest Fire, Heatwave and Forest Fire*, and *Drought, Heatwave, and Forest Fire.*

Within the one-coupling models the influence of one hazard driver is considered when defining the modelling parameters of the other hazard. For the case of pluvial flooding with storm surge. The outputs from the storm surge model are utilised to define the boundary conditions for the pluvial flood model. Within the scope of the flooding with extreme wind model, potential effects of extreme wind events on surface flows will be considered such as how the accumulation of debris during or following an extreme wind event can block flow pathways resulting in greater risks of flooding.

For the statistical analysis of hazard drivers the climate data is analysed to select climate input parameters where the definition of one hazard occurs within the timeframe of another hazard. For instance, for the heatwave and drought model the selected scenarios for modelling within a region will first identify (from climate data) periods of time that a modelled region is within drought and then identify scenarios within these drought periods that can be defined as heatwaves as per the extreme event definitions in ***Table 7***. For the other multi-hazard scenarios whereby Forest Fire is one of the featured hazards, as the FWI index shares climate input data that is a component of the other hazards to be modelled in combination such as Temperature, Precipitation and Wind (see ***Figure 38***) a similar statistical approach is used such as extreme wind during forest, forest fire during drought, forest fire during heatwave, and forest fire during a heatwave that is occurring during a drought. Within each of these models the influence of the hazards with respect to the derived FWI scores is analysed.

This project has received funding from the European Union's Horizon Europe research and innovation programme under grant agreement No. 101093806. The publication reflects only the authors' views and the European Union is not liable for any use that may be made of the information contained therein.

For the Joint Probability assessment, the work outlined within this deliverable highlights two main approaches for the quantification and visualisation of compound coincident and compound consecutive hazards.

The first approach highlighted is the use of statistical analysis of climate data whereby the probability of respective compound hazard drivers such as extreme wind and rainfall occurring either in the same place at same time or one within a pre-defined time frame of the other in the same location is assessed. By considering multiple climate models and SSPs the modelling framework defines a most likely compound hazard scenario for given return periods utilising the median values of the respective driver along with a degree of the uncertainty through the selection of the 90th percentiles to define more potential extremes for the selected return periods.

The second approach highlights the use of Copulas as a means of defining relationships between two or more independent variables. Through analysis of climate data and the use of python libraries such as Copulae; large amounts of synthetic data can be generated that can be utilised to define the probability of compound events. This mathematical approach of generating synthetic data is of particular use when data relating to the extremes of compound scenarios is limited.

In summary the modelling approaches developed in task 2.3 and outlined within this document provide a guide/framework for setting up modelling tools for modelling multi-hazard scenarios and provide a basis for the selection criteria of input parameters required for the modelling of return periods that are of interest to the case studies.

6.2 Lessons learned

The bivariate Copula Assessment approach requires representative datasets that describe the key features of events, which will be critical for capturing the relationship between multi hazards. The attributes are more than the intensity or magnitude of single hazards. The timing and duration of hazards, and the lag between consecutive hazards are also important factors to be incorporated into the analysis. In the study, the 7-day and 30-day time window were assumed to compare the difference of consecutive events against coincident events. The size of time window, and the duration of events may require further analysis to better estimate the joint probability of such events.

Using specific combinations of hazard variables as the thresholds for evaluating the joint probability will only pick up the conditions that both variables are above or below the thresholds. This may have limited effect when quantifying extreme conditions but will not be able to cover the full spectrum of moderate events. In addition, no uniform criteria are applicable for the selections of thresholds in different areas. Each location will require detailed analysis to determine adequate thresholds that represent the unique hazard attributes in the region.

Once the attributes are well reflected in the analysis, it is possible to create synthetic datasets for simulating the possible combinations of compound or consecutive hazards. Nevertheless, the copula approach was able to analyze the relationship between two hazard variables. To evaluate the relationship between three variables at the same time was challenging and complicated. Thus, the analysis was done in paired variables.

This project has received funding from the European Union's Horizon Europe research and innovation programme under grant agreement No. 101093806. The publication reflects only the authors' views and the European Union is not liable for any use that may be made of the information contained therein.

While the observation data were insufficient for using the copula method, the JOIN-SEA methodology was applied to evaluate the joint annual probability of between two hazard variables. The assumptions of the correlation between the variables were made to test the plausible range of joint probability.

DRAFT

This project has received funding from the European Union's Horizon Europe research and innovation programme under grant agreement No. 101093806. The publication reflects only the authors' views and the European Union is not liable for any use that may be made of the information contained therein.

References

Andrews, P.L., Loftsgaarden, D.O., Bradshaw, L.S. (2003). Evaluation of fire danger rating indexes using logistic regression and percentile analysis. International Journal of Wildland Fire, 12, 213–226.

Azevedo de Almeida, B., & Mostafavi, A. (2016). Resilience of infrastructure systems to sea-level rise in coastal areas: Impacts, adaptation measures, and implementation challenges. Sustainability, 8(11), 1115.

Bevacqua, E., Maraun, D., Vousdoukas, M. I., Voukouvalas, E., Vrac, M., Mentaschi, L., & Widmann, M. (2019). Higher probability of compound flooding from precipitation and storm surge in Europe under anthropogenic climate change. Science Advances, 5(9).

Bok, D., (2025). Copulae, https://copulae.readthedocs.io/en/latest/

Crisi-Adapt II. (2020). Deliverable 3.1: Description of tools for modeling climate related impacts.

de Ruiter, M.C., Couasnon, A., van den Homberg, M.J.C., Daniell, J.E., Gill, J.C., Ward, P.J., 2020. Why We Can No Longer Ignore Consecutive Disasters. Earth's Future 8, e2019EF001425. https://doi.org/10.1029/2019EF001425

Domingo, N. D. S., Paludan, B., Madsen, H., Hanses, F., & Mark, O. (2010). Climate Change and Storm Surges: Assessing Impacts on Your Coastal City Through Mike Flood Modeling. DHI Group.

Franzke, C., 2017. Impacts of a Changing Climate on Economic Damages and Insurance. Economics of Disasters and Climate Change 1. https://doi.org/10.1007/s41885-017-0004-3

Gill, J.C., Malamud, B.D., 2014. Reviewing and visualizing the interactions of natural hazards. Rev. Geophys. 52, 680–722.

Hawkes, P.J., Svensson, C., 2005. Joint Probability: Dependence Mapping and Best Practice: Technical report on dependence mapping (No. R&D Technical Report FD2308/TR1). Defra - Flood Management Division, London, UK.

Hielkema, L., Suidman, J., Jaime, C., 2021. Multi-Hazard Risk Analysis Methodologies. URL https://www.anticipation-hub.org/news/multi-hazard-risk-analysis-methodologies (accessed 6.27.24).

ICARIA. (2023a). Deliverable 1.2: Climate Projections and Hazard Scenarios

ICARIA. (2023b). Deliverable 2.1: Holistic modeling framework for multi-hazard events.

Jo, J., Kim, S., Mase, H., Mori, N., & Tsujimoto, G. (2021). Development of a coupled coastal flood model of surge, wave, precipitation and sewer backflow for urban areas. Journal of Japan Society of Civil Engineers, Ser. B2 (Coastal Engineering), 77(2), I_253-I_258.

Karavitis, C.A.; Tsesmelis, D.E.; Skondras, N.A.; Stamatakos, D.; Alexandris, S.; Fassouli, V.; Vasilakou, C.G.; Oikonomou, P.D.; Gregorič, G.; Grigg, N.S.; et al. Linking Drought Characteristics to Impacts on a Spatial and Temporal Scale. Water Policy 2014, 16, 1172–1197, doi:10.2166/wp.2014.205

This project has received funding from the European Union's Horizon Europe research and innovation programme under grant agreement No. 101093806. The publication reflects only the authors' views and the European Union is not liable for any use that may be made of the information contained therein.

Kim, D. J., Song, Y. H., & Lee, J. H. (2023). Potential Performance Assessment of Coastal Urban Sewer Network according to Sea Level Rise. Journal of the Korean Society of Hazard Mitigation, 23(1), 199-208.

Laster Grip, I., Haghighatafshar, S., & Aspegren, H. (2021). A methodology for the assessment of compound sea level and rainfall impact on urban drainage networks in a coastal city under climate change. City and Environment Interactions, 12.

Lee, S., Kang, T., Sun, D., & Park, J. J. (2020). Enhancing an analysis method of compound flooding in coastal areas by linking flow simulation models of coasts and watershed. Sustainability, 12(16), 6572.

Long, Z. Y., & Gao, L. (2023). Estimating the combined risks of sea level rise and storm surges using a numerical model: Application to Macao. Journal of Cleaner Production, 407, 137155.

McKee, T.B., N.J. Doesken and J. Kleist. (1993). The relationship of drought frequency and duration to time scale. In: Proceedings of the Eighth Conference on Applied Climatology, Anaheim, California, 17–22 January 1993. Boston, American Meteorological Society, 179–184.

Meyers, S. D., Landry, S., Beck, M. W., & Luther, M. E. (2021). Using logistic regression to model the risk of sewer overflows triggered by compound flooding with application to sea level rise. Urban Climate, 35, 100752

Ming, X., Liang, Q., Dawson, R., Xia, X., & Hou, J. (2022). A quantitative multi-hazard risk assessment framework for compound flooding considering hazard inter-dependencies and interactions. Journal of Hydrology, 607, 127477

Montalvo, C., Reyes-Silva, J. D., Sañudo, E., Cea, L., & Puertas, J. (2024). Urban pluvial flood modelling in the absence of sewer drainage network data: A physics-based approach. Journal of Hydrology, 634, 131043.

Owen, L. E., Catto, J. L., Stephenson, D. B., & Dunstone, N. J. (2021). Compound precipitation and wind extremes over Europe and their relationship to extratropical cyclones. Weather and Climate Extremes, 33, 100342.

Pacey, G.P., Schultz, D.M., Garcia-Carreras, L., 2021. Severe Convective Windstorms in Europe: Climatology, Preconvective Environments, and Convective Mode. Weather and Forecasting 36, 237–252. https://doi.org/10.1175/WAF-D-20-0075.1

Páscoa, P., Gouveia, C.M., Ribeiro, A.F.S., Russo, A., 2024. Compound drought and hot events assessment in Australia using copula functions. Environ. Res. Commun. 6, 031002. https://doi.org/10.1088/2515-7620/ad2bb8

Qiang, Y., He, J., Xiao, T., Lu, W., Li, J., & Zhang, L. (2021a). Coastal town flooding upon compound rainfall-wave overtopping-storm surge during extreme tropical cyclones in Hong Kong. Journal of Hydrology: Regional Studies, 37, 100890.

This project has received funding from the European Union's Horizon Europe research and innovation programme under grant agreement No. 101093806. The publication reflects only the authors' views and the European Union is not liable for any use that may be made of the information contained therein.

Qiang, Y., Zhang, L., He, J., Xiao, T., Huang, H., & Wang, H. (2021b). Urban flood analysis for Pearl River Delta cities using an equivalent drainage method upon combined rainfall-high tide-storm surge events. Journal of Hydrology, 597, 126293.

Richardson, D., Black, A.S., Irving, D. et al. Global increase in wildfire potential from compound fire weather and drought. npj Clim Atmos Sci 5, 23 (2022). https://doi.org/10.1038/s41612-022-00248-4

Santiago-Collazo, F. L., Bilskie, M. V., & Hagen, S. C. (2019). A comprehensive review of compound inundation models in low-gradient coastal watersheds. Environmental Modelling & Software, 119, 166-181.

Scott, J.H., Burgan, R.E. (2005). Standard fire behavior fuel models: a comprehensive set for use with Rothermel's surface fire spread model. Gen. Tech. Rep. RMRS-GTR153. U.S. Department of Agriculture, Forest Service, Rocky Mountain Research Station, Fort Collins, CO.

Sutanto, S.J., Vitolo, C., Napoli, C.D., D'Andrea, M., Lanen, H.A.J.V., 2020. Heatwaves, droughts, and fires: Exploring compound and cascading dry hazards at the pan-European scale. Environment International 134, 105276. https://doi.org/10.1016/j.envint.2019.105276

UNDRR. (2020). The Human Cost of Disasters: An Overview of the Last 20 Years (2000–2019). Geneva, Switzerland.

Van Wagner, C.E.; Pickett, T.L. Equations and FORTRAN Program for the Canadian Forest Fire Weather Index System; 1985;

Varela, V., Sfetsos, A., Vlachogiannis, D., & Gounaris, N. (2018). Fire Weather Index (FWI) classification for fire danger assessment applied in Greece. Tethys, 15, 31-40.

Zong, X., Yin, Y., Yin, M., Hou, W., Deng, H., & Cui, T. (2023). Occurrence and hotspots of multivariate and temporally compounding events in China from 1961 to 2020. NPJ Climate and Atmospheric Science, 6(1), 168.

Zscheischler, J., Westra, S., Van Den Hurk, B. J., Seneviratne, S. I., Ward, P. J., Pitman, A., ... & Zhang, X. (2018). Future climate risk from compound events. Nature climate change, 8(6), 469-477.

This project has received funding from the European Union's Horizon Europe research and innovation programme under grant agreement No. 101093806. The publication reflects only the authors' views and the European Union is not liable for any use that may be made of the information contained therein.

Annex 1: Data Management Statement

Table A.1. Data used in preparation of ICARIA Deliverable 2.4.

Dataset name	Format	Size	Owner and re-use conditions	Potential utility within and outside ICARIA	Unique ID
ICARIA D2.4 inputs	CSV files	99 MB	CC by	Further analysis of joint probability for multi hazards	https://10.5281/zenodo.17402259

Table A.2. Data produced in preparation of ICARIA Deliverable 2.4.

Dataset name	Format	Size	Owner and re-use conditions	Potential utility within and outside ICARIA	Unique ID
ICARIA D2.4	CSV, TXT, PNG, XLS, HTML	736 MB	CC by	Further analysis of joint probability for multi hazards	https://doi.org/10.5281/zenodo.17402070

DRAFT

This project has received funding from the European Union's Horizon Europe research and innovation programme under grant agreement No. 101093806. The publication reflects only the authors' views and the European Union is not liable for any use that may be made of the information contained therein.

DRAFT

More info: ***www.icaria-project.eu***